



Estimates of critical loads and exceedances of acidity and nutrient nitrogen for mineral soils in Canada for 2014–2016 average annual sulfur and nitrogen atmospheric deposition

Hazel Cathcart¹, Julian Aherne², Michael D. Moran^{1,☆}, Verica Savic-Jovicic¹, Paul A. Makar¹, and Amanda Cole¹

¹Air Quality Research Division, Atmospheric Science and Technology Directorate, Science and Technology Branch, Environment and Climate Change Canada, Toronto, Ontario, M3H 5T4, Canada

²School of the Environment, Trent University, Peterborough, Ontario, K9L 0G2, Canada

☆retired

Correspondence: Hazel Cathcart (hazel.cathcart@ec.gc.ca)

Received: 26 July 2024 – Discussion started: 8 August 2024

Revised: 29 October 2024 – Accepted: 4 November 2024 – Published: 30 January 2025

Abstract. The steady-state simple mass balance model was applied to natural and semi-natural terrestrial ecosystems across Canada to produce nation-wide critical loads of acidity (maximum sulfur, $CL_{\max S}$; maximum nitrogen, $CL_{\max N}$; minimum nitrogen, $CL_{\min N}$) and nutrient nitrogen ($CL_{\text{nut}N}$) at 250 m resolution. Parameterisation of the model for Canadian ecosystems was considered with attention to the selection of the chemical criterion for damage at a site-specific resolution, with comparison between protection levels of 5 % and 20 % growth reduction (approximating commonly chosen base-cation-to-aluminum ratios of 1 and 10, respectively). Other parameters explored include modelled base cation deposition and site-specific nutrient and base cation uptake estimates based on North American tree chemistry data and tree species and biomass maps. Critical loads of acidity were estimated to be low (e.g., below $500 \text{ eq. ha}^{-1} \text{ yr}^{-1}$) for much of the country, particularly above 60° N latitude, where base cation weathering rates are low due to cold annual average temperature. Exceedances were mapped relative to annual sulfur and nitrogen deposition averaged over 2014–2016. Results show that under a conservative estimate (5 % protection level), 10 % of Canada's protected and conserved areas in the study area experienced exceedance of some level of the soil critical load of acidity, while 70 % experienced exceedance of the soil critical load of nutrient nitrogen.

Copyright statement. ©His Majesty the King in Right of Canada, as represented by the Minister of Environment and Climate Change Canada, 2024.

1 Introduction

During the last 3 decades, reductions in sulfur (S) and nitrogen (N) deposition have led to improvements in ecosystem health across the US and Canada; nonetheless, the acid rain question remains relevant in Canada. Large point sources of emissions in western Canada have emerged, prompting concerns of impacts to sensitive ecosystems in British Columbia and the Athabasca oil sands region (AOSR) in northeastern Alberta (e.g., Mongeon et al., 2010; Williston et al., 2016; Makar et al., 2018). Further, increased marine traffic in the Arctic due to the effects of anthropogenic warming has raised questions about potential impacts of acidic deposition on northern ecosystems already under pressure from climate change (Forsius et al., 2010; Liang and Aherne, 2019). The recovery of forest soils from decades of elevated acidic deposition in the northeastern US and eastern Canada is encouraging but is predicted to be slow (Lawrence et al., 2015; Hazlett et al., 2020) and is complicated by the effect of elevated N deposition (Clark et al., 2013; Simkin et al., 2016; Pardo et al., 2019; Wilkins et al., 2023) and climate change (Wu and Driscoll, 2010). The importance of N deposition to acidification and eutrophication has received increased recognition in recent years, prompting new avenues of risk assessment and

mapping (e.g., empirical critical loads of nitrogen; Bobbink et al., 2022; Bobbink and Hicks, 2014). While N oxide emissions in Canada declined by 41 % between 1990 and 2022, ammonia emissions increased by 24 % in that same period (ECCC, 2024).

The critical load concept, defined as “the maximum deposition that will not cause chemical changes leading to long-term harmful effects on ecosystem structure and function” (Nilsson and Grenfelt, 1988), is the primary tool for identifying ecosystems that are sensitive to air pollution, particularly with respect to acidification and eutrophication (De Vries et al., 2015; Burns et al., 2008). Ecosystems that receive deposition above their critical load are said to be in exceedance; i.e., they are at risk of undergoing biological damage. Soil acidification is characterised by attrition of base cations and a decrease in soil pH, which in turn causes leaching of toxic metals, such as aluminum, and damage to plant roots. During the past 3 decades, these effects have been observed in forest soils in the northeastern US and eastern Canada (e.g., Cronan and Schofield, 1990; Likens et al., 1996; Lawrence et al., 1999) that received acidic deposition in excess of their critical loads. The effects of nutrient N on ecosystems, which include eutrophication, reduced plant biodiversity, and plant community changes, have also become an emerging issue, with studies suggesting that some Canadian ecosystems are in exceedance of their nutrient N critical load (e.g., Aherne and Posch, 2013; Reinds et al., 2015; Williston et al., 2016).

The standard approach for estimating soil critical loads is the simple mass balance (SMB) model (Sverdrup and De Vries, 1994; Posch et al., 2015), a steady-state soil chemistry model with several simplifying assumptions to reduce input requirements. This approach has been used for regional and provincial critical load assessments in Canada (e.g., Ouimet et al., 2006; Aklilu et al., 2022) as well as on a multi-provincial (NEG-ECP, 2001; Carou et al., 2008; Aherne and Posch, 2013) and national scale (Reinds et al., 2015). However, nationwide implementations of the SMB model in Canada have been challenged by data paucity and incompatibility across provinces (i.e., different data sources, methodology, and spatial alignment), coarse input map resolution, and computational difficulties driven by the size of the country and the subsequent size of data files used in critical load calculations. In recent years, though, high-resolution input data (for soils, meteorology, and forest composition) have become available and present an opportunity to refine, expand, and harmonise critical loads across the entire country, including extending maps into the Canadian Arctic. These developments come at a time when policymakers in Canada are seeking to define and track air-quality impacts (such as those by acidic S and N deposition) on sensitive ecosystems under the Addressing Air Pollution Horizontal Initiative (ECCC, 2021). Furthermore, the development of high-resolution critical loads of nutrient N to assess terrestrial eutrophication risk may contribute to efforts to meet biodiversity goals such as those under the Kunming–Montreal

Global Biodiversity Framework (ECCC, 2023c). While the SMB model is a well-established and widely used approach to determine critical loads, there remains a need for harmonised application across Canadian ecosystems to provide maps from which the effects of S and N deposition can be assessed.

The objective of this study was to assess the impacts of acidic (S and N) and nutrient N deposition on terrestrial ecosystems Canada-wide using the critical loads framework. In doing so, we applied a harmonised methodology to the SMB model for Canadian ecosystems using high-resolution input maps, including modelled Canada-wide base cation deposition (crucial for the estimation of critical loads). We also explored the choice of chemical (damage) criteria for Canadian ecosystems using a site-specific approach. Finally, we assessed the impact of anthropogenic base cation deposition on exceedance estimates under annual average S and N deposition (ECCC, 2023a) for the 3-year period from 2014–2016, using the Canadian Protected and Conserved Areas Database (CPCAD; ECCC, 2023b), to evaluate risk to sites that may be of interest to policymakers.

2 Methods

2.1 Study area

As the second-largest country by landmass in the world at over 9.9×10^6 km², Canada is home to a variety of climates, soils, vegetation, and geological structures that are grouped into distinct ecozones which are often used to generalise critical loads across similar ecosystems (Fig. 1a). The full extent of Canada was included in this study to bring together estimates for all 10 provinces and 3 territories. However, only natural and semi-natural soils meeting certain criteria for critical load estimations were considered. A land cover map (CEC, 2018) was used to exclude non-soil ecosystems including water, wetlands, and permanent snow and ice (see Fig. 1b). Soils were further limited to natural and semi-natural ecosystems by excluding urban areas, crop classes, and areas within the boundaries of the agricultural ecumene (Fig. 1b). Areas considered “barren” by land classification were not excluded when mineral soil depth was indicated in the interest of including as much of the Arctic region as possible; as the Arctic may be greening under global climate change (Myers-Smith et al., 2020) and northern shipping routes become viable, the question of ecosystem health in this region becomes more material. Since peat and wetland soil classification is difficult at a Canada-wide scale (i.e., data at the required scale are presently unavailable), and given that the satellite land cover map underestimates wetland cover (3.7 % versus an expected 13 % as given by the National Wetlands Working Group, 1997), organic soils with 30 % or more organic matter content were filtered out to close this gap. The Hudson Plain ecozone, which contains

the world's largest contiguous wetland and is 80 % wetland by cover (ECCC, 2016), was also broadly excluded from the study because of low mineral soil presence.

2.2 The simple mass balance model for acidity and nutrient nitrogen

Critical loads of acidity were estimated using the SMB model, which balances sources, sinks, and outflows of S and N in terrestrial ecosystems while assuming ecosystems are at long-term equilibrium (i.e., about 100 years, representing at least one forest rotation cycle) (CLRTAP, 2015). The SMB model defines the critical load of S and N acidity (Fig. 2) as a function of the maximum S critical load ($CL_{\max}S$), the maximum N critical load ($CL_{\max}N$), and the amount of N taken up by the ecosystem ($CL_{\min}N$). Pairs of S and N deposition that fall outside this function (white area, Fig. 2) signify that the receiving ecosystem is in exceedance of its critical load of acidity (i.e., it receives a potentially damaging amount of acidic deposition). Exceedance calculations are divided into four regions to determine the shortest path to the critical load line along the function.

The determination of $CL_{\max}S$ requires knowledge of non-sea-salt base cation (calcium, magnesium, potassium, sodium) deposition (BC_{dep}), soil base cation weathering (BC_{we}), chloride deposition (Cl_{dep}), base cation uptake (Bc_{up}), and the critical leaching of acid neutralising capacity (the ability of the ecosystem to buffer incoming acidity, denoted $ANC_{\text{le,crit}}$; see Eq. 1). Note that sodium is included in some base cation terms (denoted BC, e.g., BC_{we}) when sodium contributes to buffering, but where it concerns uptake by vegetation sodium is omitted since it is non-essential to plants (denoted Bc, e.g., Bc_{up}).

$$CL_{\max}S = BC_{\text{dep}} + BC_{\text{we}} - Cl_{\text{dep}} - Bc_{\text{up}} - ANC_{\text{le,crit}} \quad (1)$$

The value of $ANC_{\text{le,crit}}$ (see Eq. 2) is determined from a critical base-cation-to-aluminum ratio (Bc / Al_{crit}), which is set to protect the chosen biota within ecosystems of interest (i.e., the critical chemical criterion), soil percolation or runoff (Q), and the gibbsite equilibrium constant (K_{gibb} ; see Sect. 2.7).

$$ANC_{\text{le,crit}} = -Q^{\frac{2}{3}} \cdot \left(1.5 \cdot \frac{BC_{\text{dep}} + BC_{\text{we}} - Bc_{\text{up}}}{K_{\text{gibb}} \cdot \left(\frac{Bc}{Al}\right)_{\text{crit}}} \right)^{\frac{1}{3}} - \left(1.5 \cdot \frac{BC_{\text{dep}} + BC_{\text{we}} - Bc_{\text{up}}}{\left(\frac{Bc}{Al}\right)_{\text{crit}}} \right) \quad (2)$$

The calculation of $CL_{\min}N$ from Eq. (3) describes the limit above which N deposition becomes acidifying, where N_u denotes N taken up by vegetation and N_i denotes long-term net immobilisation of N in the root zone of soils under steady-state conditions. A value of $35.7 \text{ eq. ha}^{-1} \text{ yr}^{-1}$ ($0.5 \text{ kg N ha}^{-1} \text{ yr}^{-1}$) was used, based on estimates of annual N_i since the last glaciation by Rosen et al. (1992) and

Johnson and Turner (2014), who recommended a range of $0.2\text{--}0.5$ and $0.5\text{--}1 \text{ kg N ha}^{-1} \text{ yr}^{-1}$, respectively; the midpoint ($0.5 \text{ kg N ha}^{-1} \text{ yr}^{-1}$) was taken as a compromise. Lastly, $CL_{\max}N$ is estimated from Eq. (4) using $CL_{\max}S$, $CL_{\min}N$, and the soil denitrification (the loss of nitrate to nitrogen gas) factor (f_{de} ; see Sect. 2.10).

$$CL_{\min}N = N_i + N_u \quad (3)$$

$$CL_{\max}N = CL_{\min}N + \frac{CL_{\max}S}{1 - f_{\text{de}}} \quad (4)$$

Equation (5) was used to estimate soil critical loads of nutrient N ($CL_{\text{nut}}N$), wherein the acceptable inorganic N leaching limit, a value set to prevent harmful effects of nutrient N such as eutrophication, vegetation community changes, nutrient imbalances, and plant sensitivity to stressors, is set from acceptable N concentrations in soil solution ($[N]_{\text{acc}}$) multiplied by Q (CLRTAP, 2015). The $[N]_{\text{acc}}$ was set to $0.0142 \text{ eq. m}^{-3}$ (0.2 mg N L^{-1} in soil solution) for conifer forests and $0.0214 \text{ eq. m}^{-3}$ (0.3 mg N L^{-1}) for all other semi-natural vegetation, following the generalised approach taken for the European critical loads database (Reinds et al., 2021), as values suggested in CLRTAP (2015) are often country-specific and do not extend to other regions or ecosystems.

$$CL_{\text{nut}}N = N_i + N_{\text{up}} + \frac{Q \times [N]_{\text{acc}}}{1 - f_{\text{de}}} \quad (5)$$

2.3 Data and mapping

Critical load estimates were calculated with the statistical programming language R version 4.1.0 (R Core Team, 2021) and the Terra package (Hijmans, 2023), wherein inputs (Table 1) to and outputs from the SMB model were represented by 250 m resolution raster maps. Alignment and projection in the World Geodetic System (WGS84) followed the layers sourced from the OpenLandMap.org project (i.e., Hengl, 2018c, a, d, b; Hengl and Wheeler, 2018; in Table 1), since they represented the majority of input (raster) data sources. Output maps were visualised using QGIS (QGIS Development Team, 2023) with accessible colour schemes (Tol, 2012). Acidity critical load components ($CL_{\max}S$, $CL_{\max}N$, $CL_{\min}N$) and $CL_{\text{nut}}N$ were all mapped using equivalents of acidity (or nutrient nitrogen) per hectare per year ($\text{eq. ha}^{-1} \text{ yr}^{-1}$).

2.4 Base cation weathering

Base cation weathering BC_{we} (i.e., calcium, magnesium, potassium and sodium) was mapped using the soil type–texture approximation method, which assigns a base cation weathering class (BC_{w0}) based on soil characteristics (organic matter, sand, and clay percentage) and the parent material acid class (see Eq. 6). A temperature correction was applied to the BC_{we} as the speed of chemical weathering can be affected by temperature. Weathering is modified by ambient temperature T , where A is the Arrhenius pre-exponential

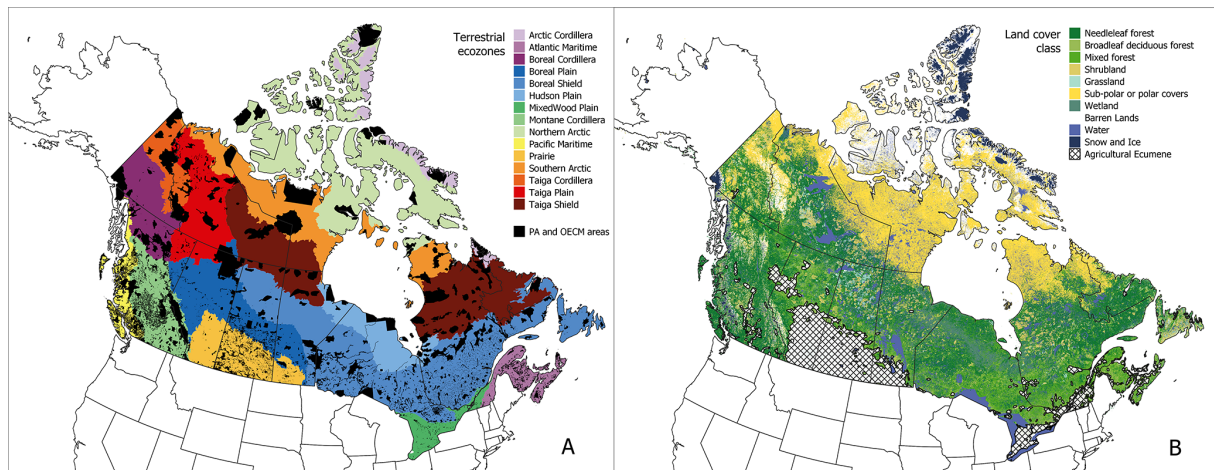


Figure 1. Study area illustrating the 15 terrestrial ecoregions of Canada (a; data source: Agriculture and Agri-Food Canada, 2013) with terrestrial protected and other effective area-based conservation measure (OECM) areas in black (ECCC, 2023b), as well as 15 (compressed to 9 for visualisation) land cover classes (b; data source: CEC, 2018) with agricultural regions in crosshatch (Statistics Canada, 2017).

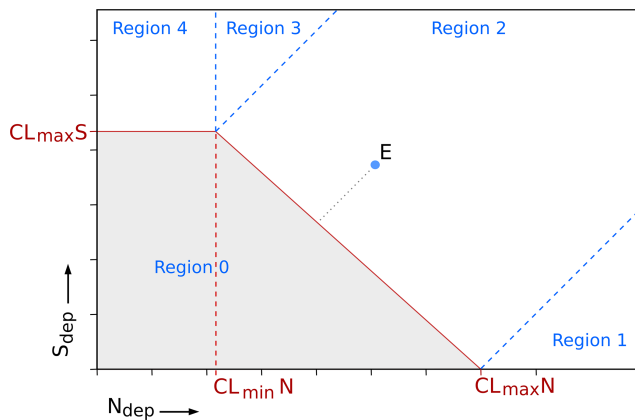


Figure 2. The acidity critical load function (red line) is defined by the maximum sulfur critical load (CL_{maxS}), the maximum nitrogen critical load (CL_{maxN}), and the minimum nitrogen critical load (CL_{minN}). Deposition points falling outside the critical load function (e.g., point E) are in exceedance (Regions 1–4), while those within the grey area (Region 0) are protected.

factor (3600 K), a temperature coefficient for soil weathering (De Vries et al., 1992; CLRTAP, 2015). Note that average annual air temperature was used to approximate annual average soil temperature in the absence of a Canada-wide soil temperature map. To address issues with resolution and continuity across provinces, high-resolution (global 250 m) predicted soil maps from the OpenLandMap.org project were used for the following input variables: bulk density (ρ), organic carbon, coarse-fragment volume (CF), and sand and clay composition (see Table 1). One of the assumptions of the SMB model is that the soil compartment is homogeneous; therefore, a weighted average for soil texture was developed based on layer depth; total depth (D); and corrections based

on coarse-fragment volume, percent organic matter, and bulk density. Percent organic matter (OM) was obtained by dividing organic carbon by 2 (Pribyl, 2010).

$$BC_{we} = \left(\frac{\rho_{soil}}{\rho_{H_2O}} \right) D \left(1 - \frac{CF}{100} \right) \left(1 - \frac{OM}{100} \right) \\ (BC_{w0} - 0.5) \times 10^{\left(\frac{A}{281} - \frac{A}{273+T} \right)} \quad (6)$$

A second assumption is that the profile depth (D) is limited to the root zone, which was set to a maximum of 50 cm for forest soils and 30 cm for other land cover types such as shrubland, grassland, and tundra. Soil depth was further limited by an absolute-depth-to-bedrock global modelled map (Hengl, 2017; Shangguan et al., 2017) in case bedrock was < 50 cm. Base cation weathering omitting sodium (BC_{we}) required for the calculation of $ANC_{le,crit}$ (Eq. 2) was scaled by 0.8 after CLRTAP (2015).

2.5 Base cation deposition

In the absence of modelled BC_{dep} data, previous Canadian mapping studies have employed a single value or a coarsely interpolated value from limited Canadian Air and Precipitation Monitoring Network (CAPMoN) stations from 1994–1998 (Aklilu et al., 2022; Carou et al., 2008; Ouimet et al., 2006). Critical load estimates for Canada by Reinds et al. (2015) used coarsely modelled global Ca deposition (Tegen and Fung, 1995) based on soil Ca content (Bowman et al., 2002) and estimated the other ions by regression. To address the gaps in data availability and spatial distribution, BC_{dep} in this study was sourced from modelled estimates produced with the Global Environmental Multiscale–Modelling Air-quality and Chemistry (GEM-MACH) model at 12 km horizontal grid spacing for the air-quality multi-model comparison project AQMEII4 (Gal-

Table 1. Data sources for input parameters to the SMB model and critical load exceedance calculation.

| Parameter | Units | Use | Original resolution | Source |
|---|---------------------------------------|---------------------------------------|---------------------|---|
| Temperature | | | | |
| Average annual air temperature (1981–2010) | °C | BC _{we} | 250 m | McKenney et al. (2006) |
| Soil | | | | |
| Absolute depth to bedrock | cm | BC _{we} | 250 m | Hengl (2017) |
| Organic carbon | × 5 g kg ⁻¹ | BC _{we} | 250 m | Hengl and Wheeler (2018) |
| Sand fraction | % | BC _{we} | 250 m | Hengl (2018c) |
| Clay fraction | % | BC _{we} | 250 m | Hengl (2018a) |
| Bulk density | g cm ⁻³ | BC _{we} | 250 m | Hengl (2018d) |
| Coarse-fragment volume | % | BC _{we} | 250 m | Hengl (2018b) |
| Parent material acid class | class | BC _{we} | 250 m | CLBBR (1996); SLCWG (2010) |
| Drainage class | class | BC _{we} | 250 m | CLBBR (1996); SLCWG (2010) |
| Runoff (Q) | mm yr ⁻¹ | ANC _{le,crit} | 0.05° × 0.1° | Reinds et al. (2015) |
| Vegetation | | | | |
| Tree species composition | % | B _{cup} , N _{up} | 250 m | Beaudoin et al. (2014) |
| Biomass | Mg ha ⁻¹ | B _{cup} , N _{up} | 250 m | Beaudoin et al. (2014) |
| Harvestable boundaries | km ² | B _{cup} , N _{up} | 250 m | Dymond et al. (2010) |
| Tree chemistry database (US) | % Ca, Mg, K, N | B _{cup} , N _{up} | – | Pardo et al. (2005) |
| Tree chemistry database (Can) | % Ca, Mg, K, N | B _{cup} , N _{up} | – | Paré et al. (2013) |
| Land cover (2010) | class | Limiting extent | 250 m | CEC (2018) |
| Agricultural ecumene (2016) | class | Limiting extent | 5 km | Statistics Canada (2017) |
| Ecozones | class | Limiting extent, summary statistics | 1 : 7.5 million | Agriculture and Agri-Food Canada (2013) |
| Deposition | | | | |
| Base cation deposition (2010, 2016) | eq. ha ⁻¹ yr ⁻¹ | ANC _{le,crit} | 12 km | Galmarini et al. (2021) |
| Total mean S and N deposition (2014–2016) | eq. ha ⁻¹ yr ⁻¹ | Exceedance | 10 km | Moran et al. (2024b, a) |
| Canadian Protected and Conserved Areas Database | class | Identifying areas of special interest | Various | ECCC (2023b) |

marini et al., 2021). Two different GEM-MACH configurations, a version with detailed parameterisations and a second version with some simplified parameterisations used for operational air-quality forecast simulations, estimated wet and dry non-sea-salt BC_{dep} for North America. Gridded annual

deposition fields for two periods, 2010 and 2016, were obtained. Ideally, emissions data sources used for S and N deposition and BC_{dep} would be the same; however, BC_{dep} is often not evaluated, and the version of the emissions inventories used for S and N deposition did not include BC_{dep}. In the

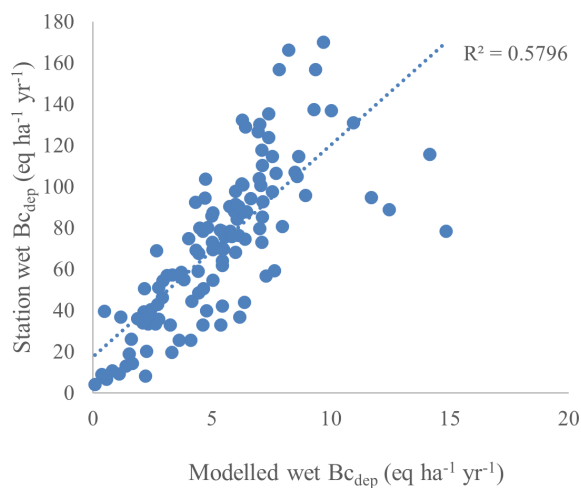


Figure 3. Modelled annual wet non-sea-salt BC_{dep} (Ca+Mg+K) versus measured annual BC_{dep} at CAPMoN and NADP stations (NADP stations limited to those within 300 m of the Canada–US border). Values are averaged across 2 years (2010 and 2016) and two model configurations. Marine station sites were corrected for sea salt contributions.

absence of a modelled Cl_{dep} map, and since the model estimates non-marine BC_{dep} , Cl_{dep} was assumed to equal sodium deposition; BC_{dep} is therefore referred to as BC_{dep} . Comparison of modelled wet BC_{dep} to measured wet BC_{dep} data from 33 Canadian Air and Precipitation Monitoring Network (CAPMoN) precipitation-chemistry stations (Feng et al., 2021) and 87 US National Atmospheric Deposition Monitoring (NADP) precipitation-chemistry stations (NADP, 2023) within 300 km of the Canada–US border showed that modelled BC_{dep} data were underestimated in each model configuration and year by an average factor of 15, though the correlation was relatively high (Fig. 3). A BC_{dep} input map was prepared by averaging (wet plus dry) BC_{dep} across the two model runs and 2 years, scaling up by 15 (after Fig. 3) and resampling to the 250 m soil grid using bilinear interpolation.

The modelled BC_{dep} and station observations include anthropogenic input, but the BC_{dep} input to the SMB model is meant to reflect long-term non-anthropogenic sources of base cations. However, large point sources of BC_{dep} (such as surface mines) are a feature of some Canadian regions, and their impact should not be overlooked in critical load assessments. Pollutant BC_{dep} from industrial sources can cause shifts in soil pH, plant community, and biodiversity, as well as direct damage to vegetation by dust (e.g., Mandre et al., 2008; Paal et al., 2013). To demonstrate the relative impact of anthropogenic sources on Canadian critical load estimates and to mitigate the impact that anthropogenic local BC_{dep} inputs have in remote regions, two scenarios were assessed, one including anthropogenic BC_{dep} and another that attempted to smooth out anthropogenic “hot spots”.

To reduce the influence of anthropogenic point sources, a smoothing filter was applied using the SAGA GIS module digital terrain model (DTM) filter to identify local areas of locally intensified BC_{dep} . Areas of BC_{dep} above a 30 % increase relative to a 20-grid radius (approximately 50 km) were removed and infilled from their edges using inverse-distance-weighted interpolation. Note that forest fire emissions may be substantial and appear as BC_{dep} hot spots; for this application of the SMB, we have not added a forest fire term to the base cation budget because of the difficulty of accounting for forest fire loss over the entire country. The loss of nitrogen due to forest fires from forest biomass and organic soil content is also significant (and not reflected in N_{up} which only deals with loss from harvesting).

2.6 Soil runoff

Soil runoff was obtained from the hydrological model MetHyd (Bonten et al., 2016) following Reinds et al. (2015). The data were resampled from the original resolution of $0.1 \times 0.05^\circ$ to 250 m, and gaps were infilled from the edges. A minimum Q was assigned ($10 \text{ m}^3 \text{ ha}^{-1} \text{ yr}^{-1}$) for broad regions where the coarse input soil map (FAO-UNESCO, 2003) used for hydrological modelling did not identify soil (i.e., exposed bedrock), but the high-resolution soil depth and texture maps used for critical loads did identify soil.

2.7 Gibbsite equilibrium constant

The gibbsite equilibrium constant (K_{gibb}) describes the relationship between free (or unbound) aluminum concentration and pH in the soil solution. As free aluminum concentrations are generally lower in the upper organic horizons, observed ranges based on the organic matter content of the soil may be used to assign a K_{gibb} value. Soils with organic matter less than 5 % were assigned a value of $950 \text{ m}^6 \text{ eq.}^{-2}$, soils with 5 %–15 % organic matter were assigned a lower value of $300 \text{ m}^6 \text{ eq.}^{-2}$, and soils ranging from 15 %–30 % organic matter were assigned a value of $100 \text{ m}^6 \text{ eq.}^{-2}$ (after CLRTAP, 2015).

2.8 Chemical criterion for damage

The critical base-cation-to-aluminum ratio (Bc / Al_{crit}) is the most widely used threshold, indicating damage to root biomass. It is a simple approach that has been used in past Canadian estimates (e.g., Carou et al., 2008). In general, it is applied as a blanket or default value (e.g., $Bc / Al_{crit} = 1$) to a range of land cover types (e.g., forest or grassland). In the current study, a species- and site-specific approach was used to assign damage thresholds for forest ecosystems based on detailed tree species maps from the 2001 Canadian National Forest Inventory (NFI) (Beaudoin et al., 2014). Two levels of protection were chosen to illustrate the difference between 20 % acceptable growth reduction (generally analogous to the default $Bc / Al_{crit} = 1$) and a 5 % growth

reduction (generally analogous to $Bc / Al_{crit} = 10$). Dose–response curves for Bc / Al_{crit} and root growth from Sverdrup and Warfvinge (1993) were matched to species present in the NFI database (Table 2). If forest was present above 25 % coverage, values were sorted by the most sensitive tree species (those with the lowest Bc / Al_{crit}) above 5 % species composition and given priority for the 250 m grid cell value. If species-specific composition data for forests (from Beaudoin et al., 2014) were not available, the Bc / Al_{crit} value was averaged to the genus; if no genus-level data were available, an average coniferous, deciduous, or mixed forest value was applied. For non-forested soils, a default value based on a representative species for the land cover type was used (e.g., 4.5 and 0.8 for 5 % and 20 % protection levels, respectively, for grassland based on the response of *Deschampsia*).

2.9 Base cation and nitrogen uptake

A species- and site-specific approach was also implemented to determine the net removal of nutrients (Ca, Mg, K, N) through tree harvesting from forest ecosystems. Base cation uptake (Bc_{up}) and N uptake (N_{up}) were estimated for forest soils by assuming stem-only removal; site-specific stand bark and trunk biomass estimates (Beaudoin et al., 2014) were multiplied by average trunk- and bark-specific nutrient and base cation concentration data from the tree chemistry databases for each species present. Two “tree chemistry” databases were merged to include as many tree species as possible (US data: Pardo et al., 2005; Canadian data: Paré et al., 2013); duplicate studies were removed from the merged database, and species data were averaged across studies. A simplifying assumption was made that stand biomass was related to the species composition (i.e., the dominant tree species in a stand is also the dominant contributor to biomass). The nutrient uptake maps were restricted to harvestable forest areas as delineated by Dymond et al. (2010), and in all other regions it was set to 0. Nutrient uptake of other land types (e.g., grasslands) was considered negligible since grazing takes place primarily in agricultural regions, which have been broadly masked out. Since Bc_{up} cannot exceed inputs from deposition, weathering, and losses from leaching, a scaling factor was used to constrain base cation uptake between its maximum (i.e., deposition plus weathering minus leaching) and a minimum calcium leaching value. The same scaling factor was applied to N_{up} .

2.10 Denitrification fraction

The soil denitrification fraction (f_{de}) is generally related to soil drainage (CLRTAP, 2015); classes ranging from excessive to very poor drainage were assigned using the Canada-wide Canadian Soil Information Service (CanSIS) databases v2.2 (CLBBR, 1996) and v.3.2 (SLCWG, 2010). Because the databases are not compatible in their geographic extent and alignment, boundary and classification priority was given to

Table 2. Species-specific Bc / Al_{crit} values for 5 % and 20 % growth reduction following Sverdrup and Warfvinge (1993). Genus-level or generalised land cover values were derived from representative species.

| Category | Bc / Al_{crit} (mol mol ⁻¹) | |
|--------------------------------|---|------|
| | 5 % | 20 % |
| Species (forest) | | |
| <i>Abies balsamea</i> | 6.0 | 1.1 |
| <i>Fagus grandifolia</i> | 1.3 | 0.6 |
| <i>Picea mariana</i> | 2.5 | 0.8 |
| <i>Pseudotsuga menziesii</i> | 4.0 | 2.0 |
| <i>Pinus strobus</i> | 1.5 | 0.5 |
| <i>Picea engelmannii</i> | 2.5 | 0.5 |
| <i>Pinus banksiana</i> | 3.0 | 1.5 |
| <i>Acer saccharum</i> | 1.3 | 0.6 |
| <i>Alnus glutinosa</i> | 4.0 | 2.0 |
| <i>Quercus rubra</i> | 1.3 | 0.6 |
| <i>Pinus ponderosa</i> | 4.5 | 2.0 |
| <i>Pinus resinosa</i> | 4.5 | 2.0 |
| <i>Picea rubens</i> | 6.0 | 1.2 |
| <i>Picea sitchensis</i> | 2.5 | 0.4 |
| <i>Larix laricina</i> | 4.0 | 2.0 |
| <i>Populus tremuloides</i> | 8.0 | 4.0 |
| <i>Tsuga heterophylla</i> | 1.0 | 0.2 |
| <i>Thuja plicata</i> | 1.0 | 0.1 |
| <i>Betula papyrifera</i> | 4.0 | 2.0 |
| <i>Picea glauca</i> | 2.5 | 0.5 |
| <i>Betula alleghaniensis</i> | 4.0 | 2.0 |
| <i>Betula populifolia</i> | 4.0 | 2.0 |
| <i>Picea abies</i> | 6.0 | 1.2 |
| <i>Pinus sylvestris</i> | 3.0 | 1.2 |
| Genus (forests) | | |
| <i>Abies</i> | 6.0 | 1.1 |
| <i>Acer</i> | 1.3 | 0.6 |
| <i>Alnus</i> | 4.0 | 2.0 |
| <i>Betula</i> | 4.0 | 2.0 |
| <i>Fagus</i> | 1.3 | 0.6 |
| <i>Larix</i> | 4.0 | 2.0 |
| <i>Picea</i> | 2.5 | 0.8 |
| <i>Pinus</i> | 3.0 | 1.5 |
| <i>Populus</i> | 8.0 | 4.0 |
| <i>Pseudotsuga</i> | 4.0 | 2.0 |
| <i>Quercus</i> | 1.3 | 0.6 |
| <i>Thuja</i> | 1.0 | 0.1 |
| <i>Tsuga</i> | 1.0 | 0.2 |
| Generalised forest | | |
| Deciduous | 4.0 | 2.0 |
| Coniferous | 3.0 | 1.2 |
| Mixed | 3.0 | 1.2 |
| Generalised land covers | | |
| Grassland | 4.5 | 0.8 |
| Scrubland | 2.8 | 0.6 |
| Tundra | 2.9 | 0.7 |

Table 3. Denitrification fraction (f_{de}) values (adapted from CLRTAP, 2015) and their corresponding drainage classifications in versions 2.2 and 3.2 of the Canadian Soil Information Service database.

| Drainage | f_{de} | V2.2 | V3.2 |
|-----------|----------|------|------|
| Excessive | 0 | E/R | VR/R |
| Good | 0.1 | W | W |
| Moderate | 0.2 | M | MW |
| Imperfect | 0.4 | I | I |
| Poor | 0.7 | P | P |
| Very poor | 0.8 | V | VP |

the most recent database version before rasterisation. Differences in classifications and their alignment to the soil drainage classes from CLRTAP (2015) are shown in Table 3.

2.11 Deposition and exceedance

Exceedances for both acidity and nutrient nitrogen were calculated using total deposition maps of annual total S and N, which were sourced from GEM-MACH model output at 10 km horizontal grid spacing (GEM-MACH v3.1.1.0, RAQDPS version 023) (Moran et al., 2025a, b). A 3-year (2014–2016) annual average was taken to reduce inter-annual variability in deposition, where input emissions based on annual emissions inventories specific to each of these 3 years were used for the three annual runs. Note that Moran et al. (2024b) have presented detailed evaluations of some components of these deposition estimates, specifically ambient concentration (as a proxy for dry deposition) and wet deposition of SO_2 and particle sulfate (pSO_4), HNO_3 and pNO_3 , and NH_3 and pNH_4 , which suggest that they are robust.

Exceedances of critical load for both acidity and nutrient nitrogen (on a 250 m grid) were summarised to the 10 km deposition grid using average accumulated exceedance (AAE), which is an area-weighted average that considers ecosystem coverage within each grid cell to derive the average of the summed exceedance; this addresses issues with sparse coverage and considers all ecosystems within the grid (Posch et al., 1999). The Canadian Protected and Conserved Areas Database (CPCAD) was used to identify areas in exceedance that may be of particular concern to policymakers (ECCC, 2023b). The database, assembled in support of Canada's reporting on Canadian Environmental Sustainability Indicators and the UN Convention on Biological Diversity (among other initiatives), identifies protected areas (PAs) such as national and provincial parks as well as other effective area-based conservation measures (OECMs). Interim areas were included in expectation of their formal establishment. Areas that fell entirely within the agricultural ecumene were removed, but areas that straddled the ecumene were retained. Areas were counted as being in exceedance if any part of the area experienced exceedance at the 250 m resolution.

The exceedance calculations used for acidity employed the methodology described by Posch et al. (2015), where the critical load function (Fig. 2) was divided into five regions, and a different formula for exceedance was used for each region. Five inputs for each 250 m grid cell were required for these calculations: the S and N total deposition pair plus $\text{CL}_{\text{max}}\text{S}$, $\text{CL}_{\text{min}}\text{N}$, and $\text{CL}_{\text{max}}\text{N}$ values. For S and N total deposition pairs falling into four of the regions, the exceedance value will be positive (i.e., in exceedance) and its magnitude indicates how great the S and N acidic deposition at the location is above the critical load for acidity. For Region 0, the exceedance value will be negative (i.e., not in exceedance) and its magnitude will give how far the S and N acidic deposition is below the critical load for acidity. The calculation of nutrient N exceedance was simply the difference between N_{dep} and $\text{CL}_{\text{nut}}\text{N}$.

3 Results

3.1 Base cation weathering

The estimated BC_{we} was very low (below $100 \text{ eq. ha}^{-1} \text{ yr}^{-1}$) for nearly all regions north of 60° N latitude and low (below $200 \text{ eq. ha}^{-1} \text{ yr}^{-1}$) for many northern regions south of 60° N latitude (Fig. 4a). Higher BC_{we} (above $500 \text{ eq. ha}^{-1} \text{ yr}^{-1}$) was predicted for the calcareous and deep soils of the Prairies and southern Ontario adjacent to agricultural regions (i.e., the mean Prairie average for natural and semi-natural soils was $714 \text{ eq. ha}^{-1} \text{ yr}^{-1}$), although most of these ecozones are excluded as part of the agricultural ecumene (Table 4). Average BC_{we} for the Arctic ecozones was $< 50 \text{ eq. ha}^{-1} \text{ yr}^{-1}$, in contrast to $\text{BC}_{\text{we}} > 700$ for Mixed Wood Plain and Prairie ecozones. Similarly, provincial averages were lowest for Nunavut and highest for Saskatchewan (Table 4). Base cation weathering without temperature correction (Fig. 4b, mean value of $570 \text{ eq. ha}^{-1} \text{ yr}^{-1}$) illustrates the strong effect temperature has on limiting BC_{we} in most of the country (average $173 \text{ eq. ha}^{-1} \text{ yr}^{-1}$), particularly Arctic and mountainous regions.

3.2 Base cation deposition

Modelled Bc_{dep} ranged from low ($< 25 \text{ eq. ha}^{-1} \text{ yr}^{-1}$) in the north to higher values ($> 200 \text{ eq. ha}^{-1} \text{ yr}^{-1}$) around the Prairies and the southern regions of the eastern provinces (Fig. 5) as well as in Alberta and Saskatchewan (Table 4). Average (smoothed) Bc_{dep} was roughly one-third of BC_{we} . Hot spots of Bc_{dep} associated with anthropogenic point sources (e.g., from mining operations as well as the contribution from the AOSR) were clearly visible in the unsmoothed map (Fig. 5a). The smoothing algorithm (Fig. 5b) eliminated most of the effects of point sources at the cost of lowering average Bc_{dep} (Canada-wide average of $68 \text{ eq. ha}^{-1} \text{ yr}^{-1}$ pre-smoothing and $52 \text{ eq. ha}^{-1} \text{ yr}^{-1}$ post-smoothing). However, it did not completely erase elevated Bc_{dep} in the AOSR; the

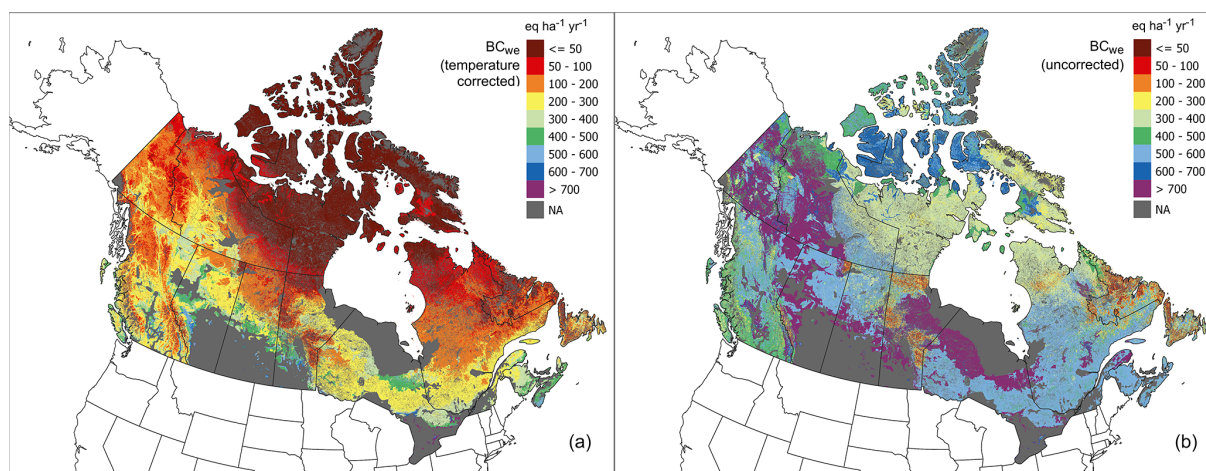


Figure 4. Base cation weathering rate (Ca+Mg+K+Na) with temperature correction (a) and without (b). The weathering rate was estimated using a soil texture approximation method with sand, clay, and parent material acid class modified by depth (see Sect. 2.4).

difference in size between other point source footprints and the AOSR necessitated a compromise in filter radius and slope selection. The smoothed Bc_{dep} was adopted as the primary data set for presenting the critical loads.

3.3 Base cation and nitrogen uptake

Base cation uptake ranged from < 1 to $545 \text{ eq. ha}^{-1} \text{ yr}^{-1}$ and was highest in coastal British Columbia; the Pacific Maritime ecozone had the highest mean Bc_{up} at $79 \text{ eq. ha}^{-1} \text{ yr}^{-1}$ (Table 4). Nitrogen uptake was also high in British Columbia and the Pacific Maritime zone (mean N_{up} of $135 \text{ eq. ha}^{-1} \text{ yr}^{-1}$) as well as the Montane Cordillera (mean N_{up} of $42 \text{ eq. ha}^{-1} \text{ yr}^{-1}$). Regions of elevated N_{up} were seen in eastern Ontario and southern Quebec (Fig. 6); these occur in the Boreal Shield ecozone, which is a large ecozone that extends across multiple provinces over which N_{up} varies (but with a mean value of $23 \text{ eq. ha}^{-1} \text{ yr}^{-1}$).

3.4 Critical base-cation-to-aluminum ratio

Almost the entire country fell below a Bc / Al_{crit} ratio of 2% under 20% root biomass growth reduction (Fig. 7a). In contrast, a Bc / Al_{crit} ratio ranged from 1–8 (average = 4.4) under the 5% root biomass growth reduction (Fig. 7b). The ratio ranged from 3–6 for forests in eastern Canada (A and B ecozones), while ranges for the Boreal Shield ecozone were 2–4 and for coastal forest in British Columbia were slightly higher at 3–4. Semi-natural grassland in the Prairies were given a ratio of 4.5 based on *Deschampsia*, but many fringe regions of the Prairies are treed and dominated by *Populus tremuloides*, which had a Bc / Al_{crit} ratio of 8.

3.5 Critical loads

The CL_{maxS} under the 20% protection level (i.e., allowing more damage) showed low sensitivity ($> 1000 \text{ eq. ha}^{-1} \text{ yr}^{-1}$) to acidic deposition for most regions below 55° N latitude (Fig. 8a). In contrast, under the 5% protection level (Fig. 8b), low sensitivity was limited to southern agricultural regions in the Prairies. The lowest CL_{maxS} and CL_{maxN} were found in the Arctic territories (Nunavut, the Northwest Territories, the Yukon; Table 4) and also Newfoundland and Labrador. Of the provinces, Quebec had the lowest CL_{maxS} ($314 \text{ eq. ha}^{-1} \text{ yr}^{-1}$) and CL_{maxN} ($299 \text{ eq. ha}^{-1} \text{ yr}^{-1}$) (Table 4). From an ecozone perspective the Mixedwood Plain ecozone had the highest CL_{maxS} at $1586 \text{ eq. ha}^{-1} \text{ yr}^{-1}$ followed by the Prairies at $1078 \text{ eq. ha}^{-1} \text{ yr}^{-1}$. The most sensitive ecozones outside the Arctic ecozones (which were below $100 \text{ eq. ha}^{-1} \text{ yr}^{-1}$) were the Boreal Cordillera and the Taiga ecozones (Table 4). For CL_{nutN} , central and northern regions of the country were sensitive to nutrient N deposition, particularly pastures, grasslands, scrublands, and sparse forest in and surrounding the Prairies (Fig. 9a). Further, very low CL_{nutN} values ($\leq 75 \text{ eq. ha}^{-1} \text{ yr}^{-1}$) were estimated over the Arctic territories (Table 4) as well as in northern Alberta and the Athabasca Basin in northern Saskatchewan. The coastal ecozones had the highest CL_{nutN} , with the Pacific Maritime and Atlantic Maritime zones having 513 and $235 \text{ eq. ha}^{-1} \text{ yr}^{-1}$, respectively. The Prairie ecozone had the lowest CL_{nutN} , lower than some of the Arctic ecozones, at $63 \text{ eq. ha}^{-1} \text{ yr}^{-1}$.

3.6 Deposition

Modelled average annual S_{dep} was below $25 \text{ eq. ha}^{-1} \text{ yr}^{-1}$ for most of the country above 59° N , as well as the Montane Cordillera ecozone that covers much of British Columbia (Fig. 10a). Southern Quebec and central On-

Table 4. Ecozone and provincial mean values for inputs and outputs of the simple mass balance model, including base cation weathering (BC_{we}), smoothed base cation deposition (Bc_{dep}), base cation uptake (Bc_{up}), nitrogen uptake (N_{up}), critical base-cation-to-aluminum ratio (Bc / Al_{crit}) for 5 % and 20 % growth reductions, average sulfur deposition (DepS) and nitrogen deposition (DepN) 2014–2017, maximum critical load of sulfur (CL_{maxS}), maximum critical load of nitrogen (CL_{maxN}), minimum critical load of nitrogen (CL_{minN}), and critical load of nutrient nitrogen (CL_{nutN}). Units are in equivalents of acidity per hectare per year ($eq. ha^{-1} yr^{-1}$) except for Bc / Al_{crit} , which is a unitless ratio. The critical loads presented in the table were calculated using the 5 % Bc / Al_{crit} and the smoothed Bc_{dep} . Note that values represent averages over eligible soils (e.g., excluding agricultural areas and organic soils).

| Ecozone | BC_{we} | Bc_{dep} | Bc_{up} | N_{up} | Bc / Al_{crit} 5 % | Bc / Al_{crit} 20 % | DepS | DepN | CL_{max} S | CL_{max} N | CL_{min} N | CL_{nut} N |
|------------------------------|-----------|------------|-----------|----------|-------------------------|--------------------------|------|------|-----------------|-----------------|-----------------|-----------------|
| Arctic Cordillera | 40 | 5 | < 1 | < 1 | 5.2 | 1.2 | 8 | 21 | 82 | 88 | 36 | 173 |
| Atlantic Maritime | 353 | 89 | 32 | 37 | 5.7 | 1.1 | 57 | 240 | 615 | 551 | 36 | 234 |
| Boreal Cordillera | 174 | 19 | 5 | 5 | 3.9 | 1.2 | 10 | 29 | 290 | 274 | 36 | 77 |
| Boreal Plain | 331 | 139 | 27 | 23 | 3.7 | 1.4 | 38 | 172 | 802 | 549 | 36 | 71 |
| Boreal Shield | 229 | 84 | 18 | 23 | 4.0 | 0.9 | 53 | 206 | 512 | 422 | 36 | 147 |
| Mixedwood Plain | 712 | 180 | < 1 | < 1 | 3.6 | 0.9 | 137 | 712 | 1586 | 1171 | 36 | 145 |
| Montane Cordillera | 240 | 52 | 39 | 42 | 3.6 | 1.2 | 25 | 98 | 447 | 473 | 40 | 164 |
| Northern Arctic | 32 | 7 | < 1 | < 1 | 5.6 | 1.3 | 9 | 20 | 63 | 75 | 41 | 75 |
| Pacific Maritime | 274 | 25 | 78 | 135 | 2.9 | 0.9 | 53 | 172 | 608 | 1281 | 48 | 513 |
| Prairie | 559 | 191 | 13 | 2 | 5.0 | 1.9 | 54 | 423 | 1078 | 893 | 59 | 63 |
| Southern Arctic | 45 | 21 | < 1 | < 1 | 5.6 | 1.3 | 10 | 26 | 112 | 118 | 60 | 65 |
| Taiga Cordillera | 106 | 31 | < 1 | < 1 | 4.3 | 1.0 | 10 | 26 | 218 | 194 | 76 | 66 |
| Taiga Plain | 195 | 51 | 4 | 4 | 3.2 | 1.0 | 13 | 37 | 390 | 246 | 79 | 51 |
| Taiga Shield | 88 | 40 | < 1 | < 1 | 3.5 | 0.8 | 18 | 54 | 227 | 200 | 192 | 110 |
| Province | | | | | | | | | | | | |
| Alberta | 285 | 133 | 24 | 17 | 3.7 | 1.4 | 35 | 142 | 730 | 512 | 58 | 78 |
| British Columbia | 235 | 37 | 40 | 53 | 3.6 | 1.2 | 26 | 92 | 439 | 551 | 91 | 206 |
| Manitoba | 217 | 86 | 7 | 7 | 2.9 | 0.9 | 41 | 146 | 512 | 338 | 44 | 66 |
| New Brunswick | 344 | 91 | 34 | 41 | 5.8 | 1.1 | 49 | 227 | 595 | 502 | 79 | 243 |
| Newfoundland and Labrador | 110 | 24 | 6 | 7 | 4.6 | 0.9 | 24 | 71 | 217 | 190 | 43 | 223 |
| Nova Scotia | 422 | 92 | 21 | 28 | 5.6 | 1.1 | 68 | 249 | 733 | 652 | 65 | 261 |
| Northwest Territories | 114 | 41 | < 1 | < 1 | 4.0 | 1.0 | 11 | 28 | 254 | 191 | 36 | 49 |
| Nunavut | 34 | 11 | < 1 | < 1 | 5.5 | 1.2 | 9 | 22 | 75 | 87 | 36 | 75 |
| Ontario | 306 | 103 | 23 | 19 | 3.8 | 0.9 | 61 | 289 | 666 | 509 | 66 | 141 |
| Prince Edward Island | 422 | 69 | 19 | 18 | 5.3 | 1.0 | 57 | 209 | 672 | 558 | 66 | 226 |
| Quebec | 148 | 46 | 11 | 14 | 4.5 | 1.0 | 38 | 132 | 314 | 299 | 50 | 153 |
| Saskatchewan | 230 | 124 | 12 | 8 | 3.1 | 1.0 | 29 | 128 | 607 | 492 | 49 | 62 |
| Yukon | 148 | 25 | < 1 | < 1 | 3.8 | 1.0 | 10 | 26 | 266 | 233 | 36 | 54 |
| Canada | 132 | 52 | 8.2 | 10 | 4.5 | 1.1 | 76 | 22 | 291 | 258 | 48 | 99 |

tario showed higher annual average values between 50–200 $eq. ha^{-1} yr^{-1}$, with some point sources showing S_{dep} in excess of 500 $eq. ha^{-1} yr^{-1}$ (e.g., at nickel smelters and mining operations in Sudbury, Ontario, and Thompson, Manitoba). Modelled average annual N_{dep} (Fig. 9b) exceeded S_{dep} in most parts of the country. A north–south N_{dep} gradient is observable in Fig. 10b, showing higher N_{dep} closer to agricultural sources in southern Ontario and Quebec and in the Prairies. Nitrogen deposition exceeding 500 $eq. ha^{-1} yr^{-1}$ was present in northern Ontario and southern Quebec as well as southern Manitoba and southwestern British Columbia.

3.7 Exceedances

Widespread but low exceedances of acidity (< 50 $eq. ha^{-1} yr^{-1}$) under average 2014–2016 deposition

were found in regions in central and southern Quebec, Ontario, Manitoba, Alberta, and British Columbia, as well as in some regions in Nova Scotia and Newfoundland, under both protection levels (Fig. 11). Further, exceedances above 200 $eq. ha^{-1} yr^{-1}$ were predicted in southern Quebec and Ontario, as well as near Winnipeg and Vancouver, under both protection levels. Exceedances of acidity under 2014–2016 S and N deposition were not generally predicted in the north. The spatial extent of exceedance was slightly greater under the 5 % protection limit as a result of lower CL_{maxS} and CL_{maxN} , particularly around point sources of S and N, such as the AOSR.

If the Bc_{dep} without smoothing is employed (i.e., the base cation deposition associated with high-magnitude anthropogenic sources is included), exceedances are reduced

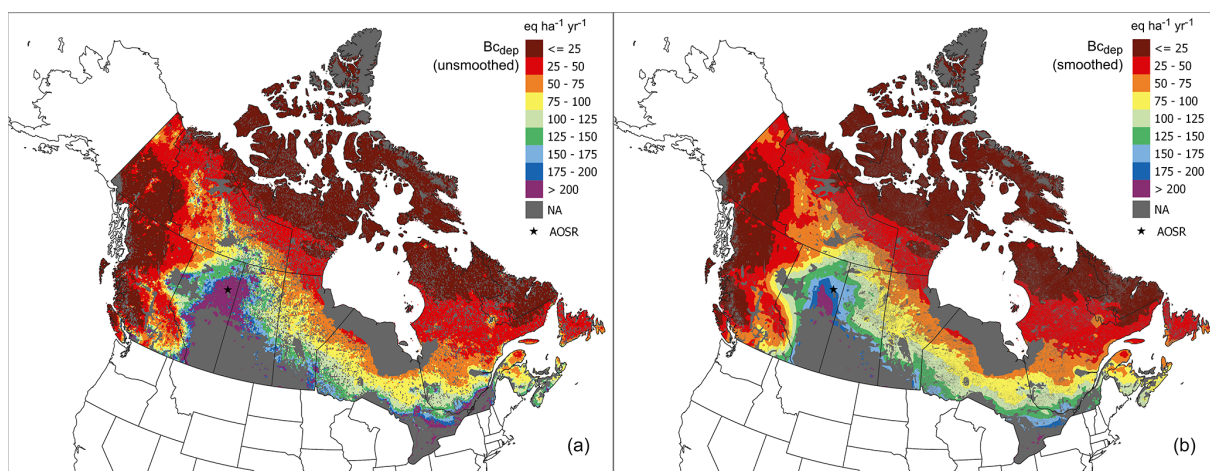


Figure 5. Non-sea-salt base cation deposition ($\text{Ca}+\text{Mg}+\text{K}$) with anthropogenic contributions (a) and after a smoothing filter was applied to reduce the effect of anthropogenic point sources (b). The location of the city of Fort McMurray within the Athabasca oil sands region (AOSR) is identified by a star.

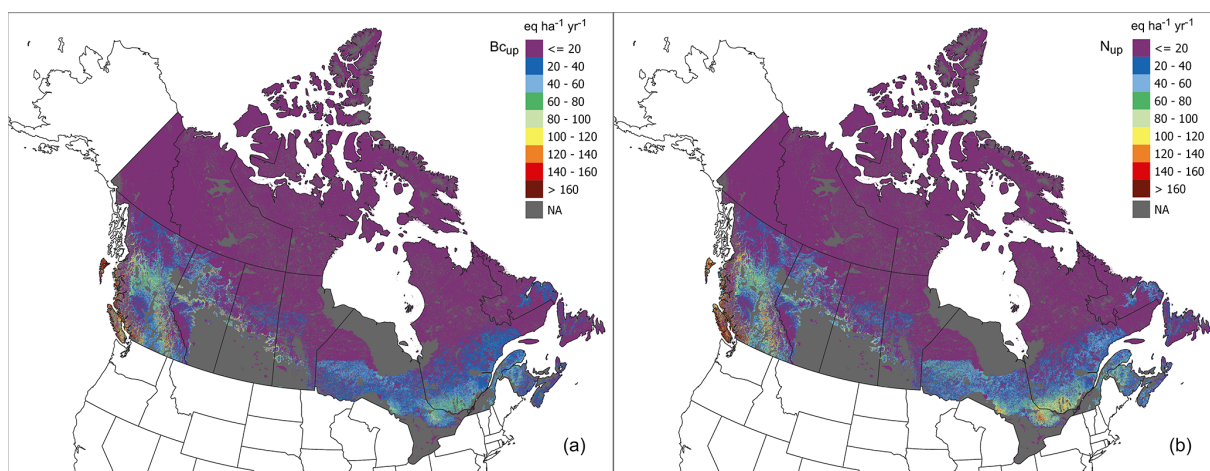


Figure 6. Base cation ($\text{Ca}+\text{Mg}+\text{K}$) uptake (a) and nitrogen uptake (b) in forested regions limited to harvestable regions (identified by Dymond et al., 2010). Uptake for non-forested ecosystems was set to 0.

(see Fig. 12b and compare to Fig. 11b). The CL_{maxS} based on anthropogenic-inclusive Bc_{dep} (at 5 % protection level; Fig. 12a) indicated that CL_{maxS} is elevated in the AOSR in comparison with the smoothed CL_{maxS} in Fig. 8b.

Widespread exceedances of CL_{nutN} were predicted across most provinces, with generally low AAE ($< 50 \text{ eq. ha}^{-1} \text{ yr}^{-1}$) extending to just north of 60° latitude, and higher values of $100\text{--}200 \text{ eq. ha}^{-1} \text{ yr}^{-1}$ were predicted from Alberta east to Quebec (Fig. 9b). Some regions adjacent to the agricultural ecumene in the Prairies, southern Ontario, Quebec, and the AOSR experienced values above 300 up to $1053 \text{ eq. ha}^{-1} \text{ yr}^{-1}$; however, 80 % of grid cells in exceedance fell below $300 \text{ eq. ha}^{-1} \text{ yr}^{-1}$.

There were 12 341 sites of interest across Canada (i.e., PA and OECM areas); however, only 8372 fall within areas assessed in this study (e.g., not within the agricultural ecumene

or Hudson Bay Plains ecozone). In total, 10 % of these sites exceeded CL_{maxS} under the 5 % protection limit (Table 5). This was roughly double the number of sites in exceedance under the 20 % protection limit. By comparison the Bc_{dep} layer with unsmoothed hot spots (i.e., retaining higher Bc_{dep} close to anthropogenic emissions areas) under the 5 % protection limit showed a reduction in total areas that are in exceedance of acidity critical loads; anthropogenic emissions of base cations reduce the exceedances by increasing N_{up} values. The number of PA and OECM sites in exceedance of CL_{nutN} was much higher – 70 % of total sites assessed (Table 5).

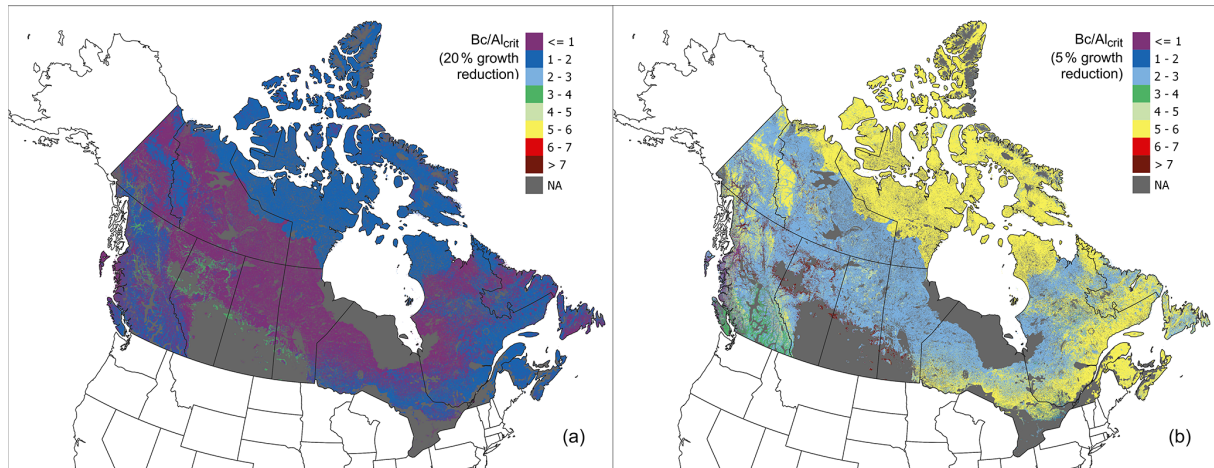


Figure 7. Critical base-cation-to-aluminum ratio (Bc / Al_{crit}) under a 20 % growth reduction (a) and a 5 % growth reduction (b). Site-specific ratios were selected for each 250 m grid cell for the most sensitive species (or genus or land-cover type if no species data available). Note that while the legends have been matched for comparison, the maximum ratio in the 20 % growth reduction map is 4.

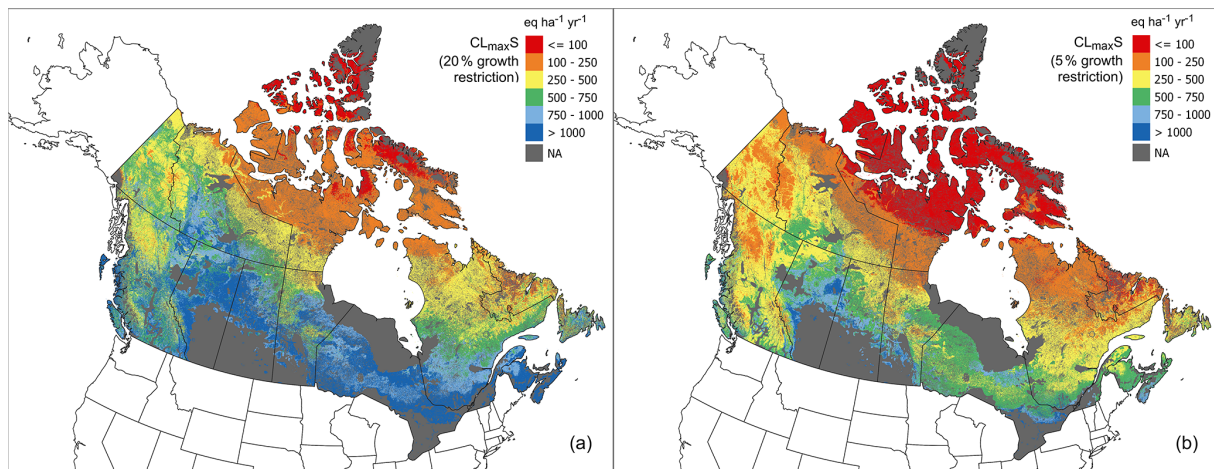


Figure 8. Maximum sulfur critical load ($CL_{max,S}$) at a 20 % growth restriction scenario (a) versus a 5 % growth restriction scenario (b), using reduced-anthropogenic (i.e., smoothed) Bc_{dep} .

4 Discussion

4.1 Uncertainties in critical loads of acidity and nutrient nitrogen

Critical loads of acidity reflect the influence of BC_{we} , particularly in the north where cold annual temperatures slow weathering rates to almost zero. However, areas near the Canada–US border also showed lower BC_{we} rates by 200–300 $eq. ha^{-1} yr^{-1}$ when corrected for temperature (Fig. 4). Soil depth remains a poorly mapped parameter that has significant impact on BC_{we} , and it is worth noting that average estimates were based on mapped soil depths (Hengl, 2017), which ranged from 1 cm to a maximum rooting depth of 30 or 50 cm. While a comparison between mapped values and site-level values is difficult (due to methodologi-

cal differences and spatial representation), there are some studies which have observational values in representative areas; for example, in northern Saskatchewan, 50 % of 107 sites were estimated below 300 $eq. ha^{-1} yr^{-1}$, slightly above our mapped estimates of 230 $eq. ha^{-1} yr^{-1}$ for (primarily northern) Saskatchewan (Table 4; Fig. 4). Estimates for conifer stands in Quebec by Ouimet et al. (2001) were 210 $eq. ha^{-1} yr^{-1}$, comparable to the mean 229 $eq. ha^{-1} yr^{-1}$ estimated for the Boreal Shield ecozone in our study (Table 4). In British Columbia, Mongeon et al. (2010) found BC_{we} to be 710 $eq. ha^{-1} yr^{-1}$, much greater than the 235 $eq. ha^{-1} yr^{-1}$ estimated in our study for the Pacific Maritime ecozone. Koseva et al. (2010) estimated BC_{we} at 10 sites in Ontario primarily in the Mixedwood Plains ecozone at 628 $eq. ha^{-1} yr^{-1}$ (compared to 306 $eq. ha^{-1} yr^{-1}$ over the Mixedwood Plains in our study). Moreover, Ko-

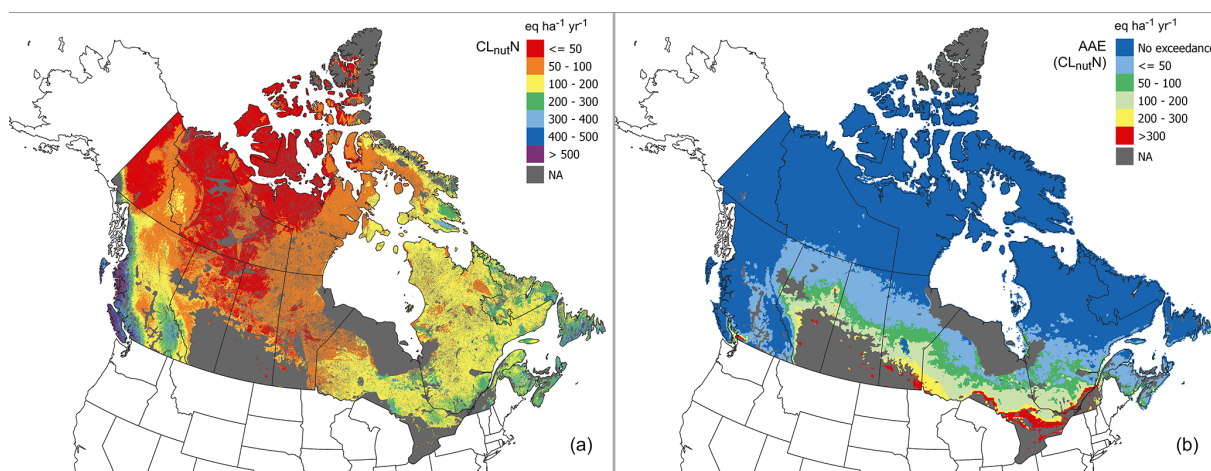


Figure 9. Critical load of nutrient nitrogen using the SMB model (a) and average accumulated exceedance of nutrient nitrogen (b) estimated under modelled total deposition of nitrogen from 2014–2016.

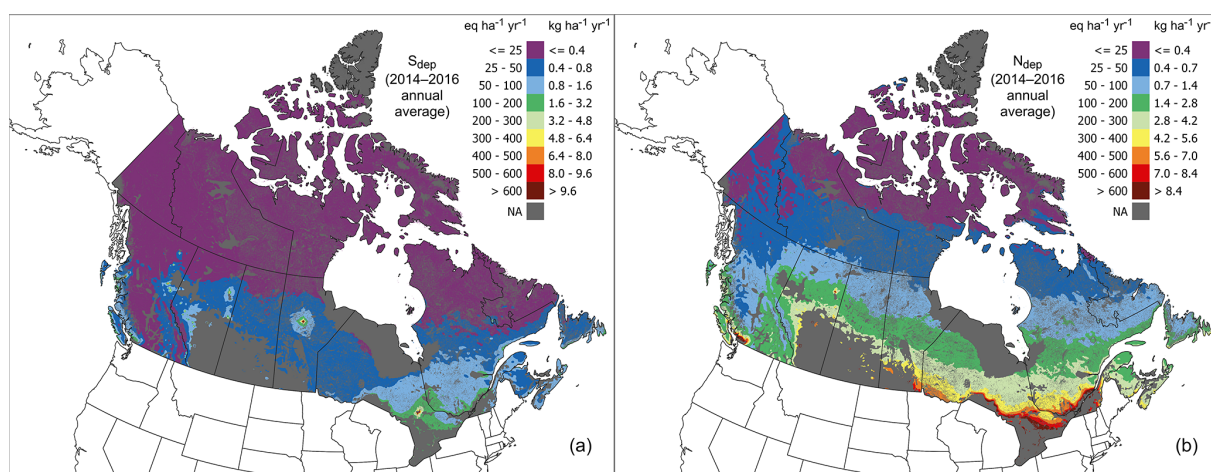


Figure 10. Modelled annual average (2014–2016) total deposition of sulfur (S_{dep} , a) and nitrogen (N_{dep} , b). Maps were sourced from GEM-MACH (Moran et al., 2025a, b).

seva et al. (2010) suggest that the soil texture approximation method (as used in our study) underestimates BC_{we} in comparison to the better-performing PROFILE model. Assessments of uncertainty in critical load estimates recognise BC_{we} as the primary driver of uncertainty (Li and McNulty, 2007; Skeffington et al., 2006), and, as such, observational data and PROFILE-modelled site data to constrain weathering rates would greatly improve critical load estimates.

While the inclusion of a modelled Bc_{dep} map represents an improvement over previous Canadian critical load projects, several factors likely contribute to the Bc_{dep} modelled negative bias (which has appeared in other publications, such as Makar et al., 2018) and may relate to how emissions processing has been carried out for air-quality models in North America. While anthropogenic emissions inventories include estimates of $PM_{2.5}$, PM_{10} , and PM_{total} mass emissions, usually only $PM_{2.5}$ and PM_{10} emissions are used in

the determination of model input emissions. However, substantial emitted base cation mass may reside in the larger size fractions (between the mass included within PM_{10} and the PM_{total}). The model version and emissions inventory data used in the base cation deposition estimates of AQMEII4 included only emissions up to $10\ \mu m$ in diameter, as did work examining emissions from multiple sources of primary particulate matter (Boutzis et al., 2020). Subsequent work using observations from the Canadian oil sands and reviewing other sources of data after Boutzis et al. (2020) and Galmarini et al. (2021) suggests that many of the same sources of anthropogenic particulate matter emissions include emitted particles between 10 and $40\ \mu m$ in diameter, the mass of which adds an additional 66 % relative to the $PM_{2.5}$ to PM_{10} “coarse-mode” emitted mass. For forest fire emissions, this additional mass is much larger. The wildfire particulate matter size distributions of Radke et al. (1988, 1990) used to

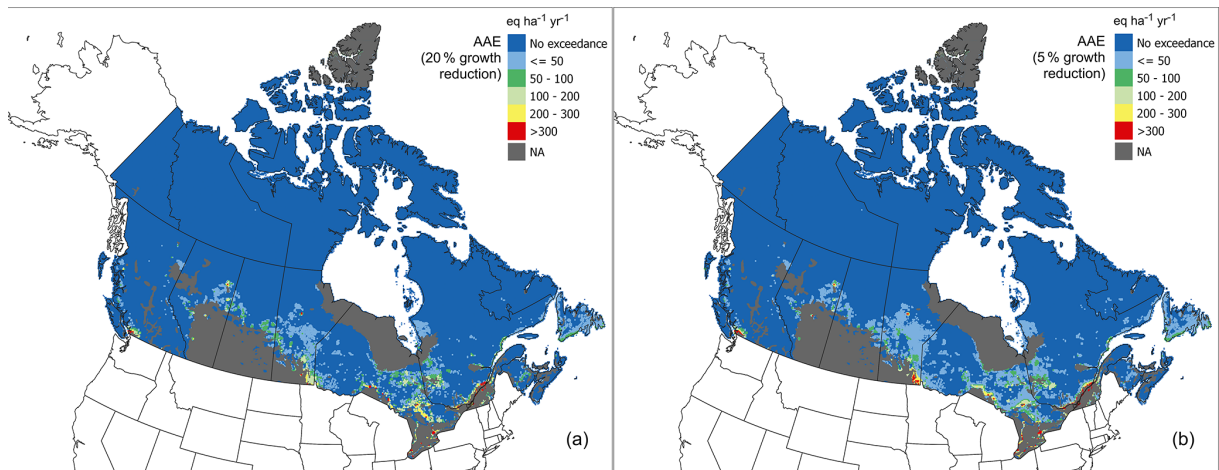


Figure 11. Average accumulated exceedance (AAE) of critical loads of acidity under 2014–2016 sulfur and nitrogen GEM-MACH-modelled deposition. Two growth reduction scenarios are presented: using a chemical criterion representing 20 % growth reduction (a) and 5 % growth reduction (b).

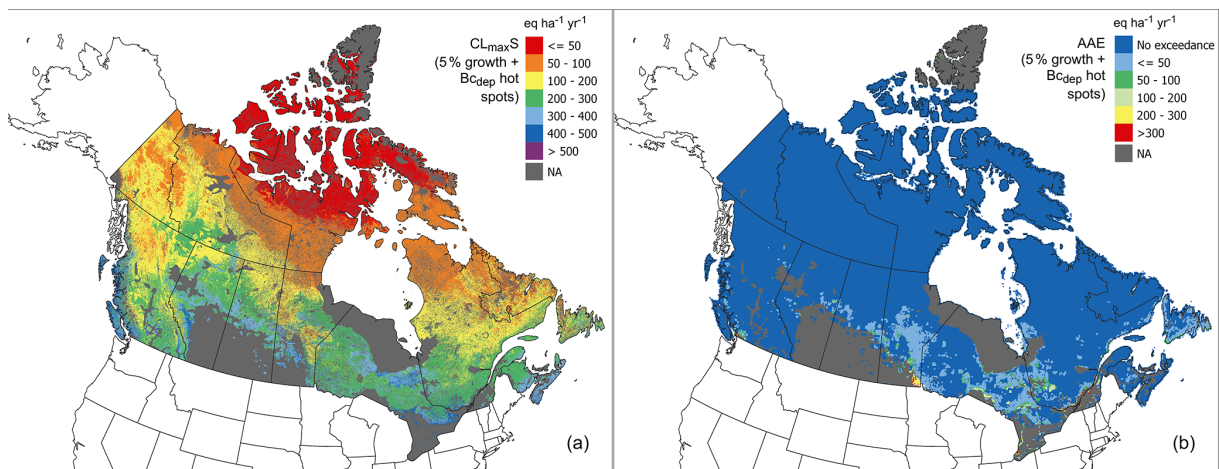


Figure 12. A scenario using base cation deposition without smoothing, illustrating the impact of hot-spot B_{cdep} on the maximum critical load of sulfur (CL_{maxS}) (a) and the average accumulated exceedance (AAE) under average 2014–2016 sulfur and nitrogen GEM-MACH-modelled deposition (b).

estimate mass up to PM_{10} in Boutzis et al. (2020) show that the emitted particle mass between 10 and $40\mu m$ in diameter is 7.26 times that emitted between $PM_{2.5}$ and PM_{10} . Approximately 9.7 % of this particle mass is composed of base cations (e.g., Table S5 of Chen et al., 2019). A third factor is another natural emission source, aeolian or wind-blown dust emissions (e.g., Bullard et al., 2016; Park et al., 2010), which was not included in the AQMEII4 simulations. These (traditionally missing) sources of base cation mass in air-quality models likely contribute to the substantial negative bias noted here. Nevertheless, regression in Fig. 3 suggests that the spatial distribution of base cation emissions and deposition from Galmarini et al. (2021) is reasonable, and we have used the relationship between modelled and observed values to provide corrected estimates of B_{cdep} .

The conservative 5 % protection level set for the B_c / Al_{crit} is favoured by the authors of the current work for critical load estimates, which affords greater ecosystem protection consistent with studies using $B_c / Al > 1$ (e.g., McDonnell et al., 2023; Mongeon et al., 2010; Ouimet et al., 2006). Historically, when acidic deposition was higher than at present, a 20 % growth reduction was a reasonable target. However, under decreasing emissions and deposition, as well as acceptable impacts to wood production, carbon storage, and ecosystem health, there is greater certainty in ecosystem protection under the 5 % protection level. It should be noted that the level of protection is a policy decision regarding how much should be protected, rather than a sensitivity one, and taking the most sensitive species through the B_c / Al_{crit} selection process ensures the highest possible

Table 5. Exceedance summarised by number of protected areas (PAs) and other effective area-based conservation measure (OECM) areas (ECCC, 2023b) experiencing any exceedance. Three exceedance scenarios are presented: critical load of acidity exceedance at 5 % and 20 % growth reduction protection levels, unsmoothed base cation deposition under the 5 % scenario, and exceedance of nutrient nitrogen (CL_{nutN}). Critical loads of acidity and nutrient nitrogen were assessed under a multi-year (2014–2016) average sulfur and nitrogen GEM-MACH-modelled total deposition.

| | PA | OECM | % exceeded |
|----------------------------------|------|------|------------|
| Number of sites | 8205 | 167 | – |
| Exceeded (5 % growth reduction) | 793 | 17 | 9.7 |
| Exceeded (20 % growth reduction) | 313 | 10 | 3.9 |
| Exceeded (5 % with hot spots) | 445 | 14 | 5.5 |
| Exceeded (CL_{nutN}) | 5807 | 85 | 70.4 |

protection based on species-specific dose–response curves. Note, however, that changes to forest health and climate may also induce pressures that are not captured in the selection of the Bc / Al_{crit} from the studies described in Sverdrup and Warfvinge (1993).

CL_{nutN} seems to be driven primarily by Q rather than by vegetation cover; low CL_{nutN} was seen in regions of correspondingly low Q values (e.g., $> 50 \text{ mm yr}^{-1}$) in much of the Arctic and central Canada. In contrast, areas with high Q were found to result in high CL_{nutN} ; as previously suggested by Reinds et al. (2015), a critical flux rather than concentration may provide more reliable critical loads in regions with elevated precipitation such as the Pacific Maritime ecozone in British Columbia.

The omission of wetlands, which cover an estimated 13 % of land in Canada, from acidity and nutrient N critical loads represents a gap in terrestrial (and aquatic) ecosystem protection. Although there are modifications to the SMB model that address critical loads for wetlands, this study was limited by the availability of a suitable national wetlands classification map. Future studies may address this data gap as wetland classification products become available.

4.2 Exceedances of critical loads

Historically, forests in eastern Canada were regarded as ecosystems most susceptible to acidification due to their underlying geology, shallow soil type, vegetation, and elevated acidic deposition from domestic and transboundary air pollution. This study adds to the body of literature supporting recent studies in both terrestrial and aquatic critical loads (e.g., Makar et al., 2018; Cathcart et al., 2016; Williston et al., 2016; Mongeon et al., 2010; Whitfield et al., 2010),

showing the likely exceedance of critical loads of acidity in central and western Canada (i.e., in regions such as Alberta, Saskatchewan, and British Columbia). The prevalence of our predicted widespread exceedances in Manitoba (Fig. 10) may reflect low mineral soil depth, as organic soil dominates this part of the country. Further, point sources (generally large mining or smelting operations) remain a concern (e.g., in southern Manitoba, the AOSR, and southern British Columbia) with regard to sharply elevated local exceedance, which may be temporally mitigated by elevated Bc_{dep} from co-located dust emission sources. Additionally, high Bc_{dep} can have an alkalinising impact on ecosystems. In China, where elevated Bc_{dep} emissions from industrialisation have historically mitigated the effects of acidic deposition in many regions, successful particle emissions mitigation strategies have reduced Bc_{dep} in recent years (as S and N deposition have declined), resulting in increased critical load exceedance (Zhao et al., 2021). However, the steady-state assumptions of the SMB require non-anthropogenic Bc_{dep} , since they must reflect long-term conditions, and base cation emissions cannot be reliably coupled with changes to those of S and N and should be considered separately.

Widespread CL_{nutN} exceedance (found in the majority of the PA and OECM sites assessed) suggests that nutrient N may present a risk to biodiversity at many sites under protective measures. However, 40 % of the grid cells showing CL_{nutN} exceedance were below $50 \text{ eq. ha}^{-1} \text{ yr}^{-1}$, and it is likely that many of these exceedances are within the uncertainty of the model. While some empirical studies of nutrient N have been done in Canada, a large knowledge gap exists for many Canadian ecosystems regarding the effect of nutrient nitrogen and its critical loads. Some work has developed Jack pine and northern ecosystems; Vandinter and Aherne (2023a) suggested that across Jack-pine-dominant forests surrounding the AOSR, the biodiversity-based empirical critical load of nutrient N was $5.6 \text{ kg ha}^{-1} \text{ yr}^{-1}$ ($400 \text{ eq. ha}^{-1} \text{ yr}^{-1}$; Vandinter and Aherne, 2023a), which is above the maximum CL_{nutN} calculated in this study within 200 km of the AOSR ($216 \text{ eq. ha}^{-1} \text{ yr}^{-1}$). Further, in low-deposition “background” regions a biodiversity-based empirical critical load of $1.4\text{--}3.15 \text{ kg ha}^{-1} \text{ yr}^{-1}$ ($100\text{--}225 \text{ eq. ha}^{-1} \text{ yr}^{-1}$) was found to protect lichen communities and other N-sensitive species in Jack pine forests across northwestern Canada (Vandinter and Aherne, 2023b); these are again higher compared to mean values in this study (e.g., for the Boreal Plain, $76 \text{ eq. ha}^{-1} \text{ yr}^{-1}$). Empirical critical loads developed for ecoregions in northern Saskatchewan (Murray et al., 2017) fall into a range of $88\text{--}123 \text{ eq. ha}^{-1} \text{ yr}^{-1}$, again higher than values suggested by this study (e.g., $62 \text{ eq. ha}^{-1} \text{ yr}^{-1}$ in Saskatchewan). In comparison to these empirical values, CL_{nutN} values in the current work are lower by a factor of 2. If CL_{nutN} is doubled, only 10 % of the soils assessed are in exceedance (versus 31 % of soils). This reduction in the areal exceedance would in turn reduce the number of PA and OECM sites in ex-

ceedance. While the spatial pattern of $CL_{nut}N$ exceedances does not generally follow exceedances of critical loads of acidity, some areas (including PA and OECM sites) in central Canada were estimated to be in exceedance of both critical loads of acidity and nutrient N, suggesting that this region may be of particular concern. Given the largest areal exceedance is of $CL_{nut}N$, observational studies with the view of expanding Canadian ecosystem empirical critical loads would help determine how, and by how much, Canadian ecosystems are affected by N_{dep} and how well these observations align with $CL_{nut}N$ in the current work. Additionally, vegetation community change-point modelling such as with the TITAN model (Baker and King, 2010) could help bring understanding to how Canadian ecosystems might experience elevated N_{dep} with regard to changes in biodiversity.

5 Conclusions

This study mapped critical loads of acidity and nutrient nitrogen for terrestrial ecosystems using the steady-state SMB model. The modelling approach used (a) high-resolution national maps of soils, meteorology, and forest composition; (b) high-resolution modelled Canada-wide Bc_{dep} ; and (c) species-specific chemical criteria for damage. The resulting national critical loads of acidity and nutrient N for Canadian terrestrial ecosystems were mapped at a 250 m resolution. The influence of different levels of protection and Bc_{dep} models was also explored, including two vegetation protection levels (5 % and 20 % root biomass growth reduction scenarios) and anthropogenic base cation deposition “hot spots”.

Terrestrial ecosystems in Canada continue to receive acidic deposition in excess of their critical loads for both acidity and nutrient N under modelled (2014–2016 average) total S and N deposition in areas of both eastern and western Canada. These areas include several major point emission sources including the Alberta oil sands region. Further, exceedance was predicted at 10 % (acidity) and 70 % (nutrient nitrogen) of the assessed sites (PA and OECM) where preserving biodiversity is a national policy goal, suggesting that current levels of N deposition may be affecting a large majority of these ecologically important sites. Soil recovery from acidic deposition is a slow process that may take decades or even centuries to reach pre-acidification levels, which cannot begin until deposition falls below critical loads. Parameterisation of the SMB model specifically for Canadian ecosystems is a step forward in refining Canadian terrestrial critical loads, and the maps produced by this study are a valuable tool in identifying and assessing regions sensitive to acidic deposition and nutrient N deposition, as well as providing a foundation for more refined provincial estimates.

Data availability. Raster files of critical load maps ($CL_{max}S$, $CL_{max}N$, $CL_{min}N$, $CL_{nut}N$) are available on the Government of

Canada’s Open Data Portal under Environment and Climate Change Canada’s records (<https://open.canada.ca/data/organization/ec>, last access: 1 October 2025) at <https://doi.org/10.18164/ec5c8bbb-3bc8-4675-a9c6-103add874b8> (Cathcart et al., 2025).

Author contributions. HC: conceptualisation, data curation, investigation, methodology, formal analysis, visualisation, writing (original draft), writing (review and editing). JA: formal analysis, methodology, writing (review and editing). MDM: data curation, investigation, methodology, writing (original draft), writing (review and editing). VSJ: data curation, investigation. PAM: investigation, methodology, writing (original draft), writing (review and editing). AC: writing (review and editing).

Competing interests. The contact author has declared that none of the authors has any competing interests.

Disclaimer. Publisher’s note: Copernicus Publications remains neutral with regard to jurisdictional claims made in the text, published maps, institutional affiliations, or any other geographical representation in this paper. While Copernicus Publications makes every effort to include appropriate place names, the final responsibility lies with the authors.

Acknowledgements. The authors wish to acknowledge Max Posch for his provision of (and guidance regarding) soil water runoff (Q) estimates and the AQMEII4 project for emissions data leading to GEM-MACH maps of base cation deposition.

Review statement. This paper was edited by Ivonne Trebs and reviewed by two anonymous referees.

References

- Agriculture and Agri-Food Canada: Terrestrial Ecozones of Canada, <https://open.canada.ca/data/en/dataset/7ad7ea01-eb23-4824-bccc-66adb7c5bdf8> (last access: 31 May 2024), 2013.
- Aherne, J. and Posch, M.: Impacts of nitrogen and sulphur deposition on forest ecosystem services in Canada, *Curr. Opin. Env. Sust.*, 5, 108–115, <https://doi.org/10.1016/j.cosust.2013.02.005>, 2013.
- Aklilu, Y.-A., Blair, L., Dinwoodie, G., and Aherne, J.: Using steady-state mass balance model to determine critical loads of acidity for terrestrial ecosystems in Alberta, Government of Alberta, Ministry of Environment and Parks, ISBN 978-1-4601-5438-0, 2022.
- Baker, M. E. and King, R. S.: A new method for detecting and interpreting biodiversity and ecological community thresholds, *Methods Ecol. Evol.*, 1, 25–37, <https://doi.org/10.1111/j.2041-210X.2009.00007.x>, 2010.
- Beaudoin, A., Bernier, P. Y., Guindon, L., Villemare, P., Guo, X. J., Stinson, G., Bergeron, T., Magnussen, S., and Hall, R. J.: Map-

- ping attributes of Canada's forests at moderate resolution through kNN and MODIS imagery, *Can. J. Forest Res.*, 44, 521–532, <https://doi.org/10.1139/cjfr-2013-0401>, 2014.
- Bobbink, R. and Hicks, W. K.: Factors Affecting Nitrogen Deposition Impacts on Biodiversity: An Overview, in: *Nitrogen Deposition, Critical Loads and Biodiversity*, edited by: Sutton, M. A., Mason, K. E., Sheppard, L. J., Sverdrup, H., Haeuber, R., and Hicks, W. K., Springer Netherlands, Dordrecht, 127–138, https://doi.org/10.1007/978-94-007-7939-6_14, 2014.
- Bobbink, R., Loran, C., and Tomassen, H.: Review and revision of empirical critical loads of nitrogen for Europe, Umweltbundesamt/German Environment Agency, Dessau-Roßlau, Germany, ISSN 1862-4804, 2022.
- Bonten, L. T. C., Reinds, G. J., and Posch, M.: A model to calculate effects of atmospheric deposition on soil acidification, eutrophication and carbon sequestration, *Environ. Model. Softw.*, 79, 75–84, <https://doi.org/10.1016/j.envsoft.2016.01.009>, 2016.
- Boutzis, E. I., Zhang, J., and Moran, M. D.: Expansion of a size disaggregation profile library for particulate matter emissions processing from three generic profiles to 36 source-type-specific profiles, *J. Air Waste Manage.*, 70, 1067–1100, <https://doi.org/10.1080/10962247.2020.1743794>, 2020.
- Bouwman, A. F., Vuuren, D. P. V., Derwent, R. G., and Posch, M.: A Global Analysis of Acidification and Eutrophication of Terrestrial Ecosystems, *Water. Air. Soil Pollut.*, 141, 349–382, <https://doi.org/10.1023/A:1021398008726>, 2002.
- Bullard, J. E., Baddock, M., Bradwell, T., Crusius, J., Darlington, E., Gaiero, D., Gassó, S., Gisladdottir, G., Hodgkins, R., McCulloch, R., McKenna-Neuman, C., Mockford, T., Stewart, H., and Thorsteinsson, T.: High-latitude dust in the Earth system, *Rev. Geophys.*, 54, 447–485, <https://doi.org/10.1002/2016RG000518>, 2016.
- Burns, D. A., Blett, T., Haeuber, R., and Pardo, L. H.: Critical loads as a policy tool for protecting ecosystems from the effects of air pollutants, *Front. Ecol. Environ.*, 6, 156–159, <https://doi.org/10.1890/070040>, 2008.
- Carou, S., Dennis, I., Aherne, J., Ouimet, R., Arp, P. A., Watmough, S. A., DeMerchant, I., Shaw, M., Vet, B., Bouchet, V., and Moran, M.: A national picture of acid deposition critical loads for forest soils in Canada, Canadian Council of Ministers of the Environment, Winnipeg, Manitoba, ISBN 978-1-896997-82-7, 2008.
- Cathcart, H., Aherne, J., Jeffries, D. S., and Scott, K. A.: Critical loads of acidity for 90,000 lakes in northern Saskatchewan: A novel approach for mapping regional sensitivity to acidic deposition, *Atmos. Environ.*, 146, 290–299, <https://doi.org/10.1016/j.atmosenv.2016.08.048>, 2016.
- Cathcart, H., Aherne, J., Moran, M. D., Savic-Jovicic, V., Makar, P. A., and Cole, A.: Critical loads of acidity (CLmaxS, CLmaxN, and CLminN) and nutrient nitrogen (CLnutN) for mineral soils in Canada, Government of Canada's Open Data Portal [data set], <https://doi.org/10.18164/ec5c8bbb-3bc8-4675-a9c6-103add874b8>, 2025.
- CEC: 2010 Land Cover of North America at 250 meters (v2.0), Commission for Environmental Cooperation (CEC), Canada Centre for Remote Sensing (CCRS), U.S. Geological Survey (USGS), Comisión Nacional para el Conocimiento y Uso de la Biodiversidad (CONABIO), Comisión Nacional Forestal (CONAFOR), Instituto Nacional de Estadística y Geografía (INEGI), <http://www.cec.org/north-american-environmental-atlas/land-cover-2010-modis-250m> (last access: 3 June 2024), 2018.
- Chen, J., Anderson, K., Pavlovic, R., Moran, M. D., Englefield, P., Thompson, D. K., Munoz-Alpizar, R., and Landry, H.: The FireWork v2.0 air quality forecast system with biomass burning emissions from the Canadian Forest Fire Emissions Prediction System v2.03, *Geosci. Model Dev.*, 12, 3283–3310, <https://doi.org/10.5194/gmd-12-3283-2019>, 2019.
- Clark, C. M., Morefield, P. E., Gilliam, F. S., and Pardo, L. H.: Estimated losses of plant biodiversity in the United States from historical N deposition (1985–2010), *Ecology*, 94, 1441–1448, <https://doi.org/10.1890/12-2016.1>, 2013.
- CLBBR: Soil Landscapes of Canada, v. 2.2, Centre for Land and Biological Resources Research, Research Branch, Agriculture and Agri-Food Canada, <https://sis.agr.gc.ca/cansis/nsdb/slc/v2.2> (last access: 3 June 2024), 1996.
- CLRTAP: Mapping critical loads for ecosystems, Chapter V of Manual on methodologies and criteria for modelling and mapping critical loads and levels and air pollution effects, risks and trends. UNECE Convention on Long-range Transboundary Air Pollution, <https://www.icpmapping.org> (last access: 3 June 2024), 2015.
- Cronan, C. S. and Schofield, C. L.: Relationships between aqueous aluminum and acidic deposition in forested watersheds of North America and northern Europe, *Environ. Sci. Technol.*, 24, 1100–1105, <https://doi.org/10.1021/es00077a022>, 1990.
- De Vries, W., Posch, M., Reinds, G. J., and Kämäri, J.: Critical loads and their exceedance on forest soils in Europe, Report 58 – The Winand Staring Centre for Integrated Land, Soil and Water Research (SC_DLO), Wageningen, the Netherlands, 123 pp., ISSN 0927-4537, 1992.
- De Vries, W., Hettelingh, J.-P., and Posch, M. (Eds.): The History and Current State of Critical Loads and Dynamic Modelling Assessments, in: *Critical loads and dynamic risk assessments: Nitrogen, acidity and metals in terrestrial and aquatic ecosystems*, Springer, 1–11, https://doi.org/10.1007/978-94-017-9508-1_1, 2015.
- Dymond, C. C., Titus, B. D., Stinson, G., and Kurz, W. A.: Future quantities and spatial distribution of harvesting residue and dead wood from natural disturbances in Canada, *Forest Ecol. Manag.*, 260, 181–192, <https://doi.org/10.1016/j.foreco.2010.04.015>, 2010.
- ECCC: Canadian Environmental Sustainability Indicators: Extent of Canada's Wetlands, ISBN 978-0-660-05390-5, 2016.
- ECCC: Evaluation of the Addressing Air Pollution Horizontal Initiative, Environment and Climate Change Canada, ISBN 978-0-660-39645-3, 2021.
- ECCC: 2022 Canadian Protected and Conserved Areas Database (CPCAD) User Manual, Environment and Climate Change Canada, <https://open.canada.ca/data/en/dataset/6c343726-1e92-451a-876a-76e17d398a1c> (last access: 1 October 2024), 2023a.
- ECCC: Canadian Protected and Conserved Areas Database 2022, Environment and Climate Change Canada, <https://www.canada.ca/en/environment-climate-change/services/national-wildlife-areas/protected-conserved-areas-database.html> (last access: 3 June 2024), 2023b.

- ECCC: Toward a 2030 Biodiversity Strategy for Canada: Halting and Reversing Nature Loss, Environment and Climate Change Canada, ISBN 978-0-660-48594-2, 2023c.
- ECCC: Canada's air pollutant emissions inventory report 1990–2022, Environment and Climate Change Canada, Gatineau, Quebec, ISSN 2562-4903, https://publications.gc.ca/collections/collection_2024/eccc/En81-30-2022-eng.pdf (last access: 25 July 2024), 2024.
- FAO-UNESCO: Digital soil map of the world and derived soil properties, CD-ROM, Rome, ISBN 978-92-3-103889-1, 92-3-103889-3, 2003.
- Feng, J., Vet, R., Cole, A., Zhang, L., Cheng, I., O'Brien, J., and Macdonald, A.-M.: Inorganic chemical components in precipitation in the eastern U.S. and Eastern Canada during 1989–2016: Temporal and regional trends of wet concentration and wet deposition from the NADP and CAPMoN measurements, *Atmos. Environ.*, 254, 118367, <https://doi.org/10.1016/j.atmosenv.2021.118367>, 2021.
- Forsius, M., Posch, M., Aherne, J., Reinds, G., Christensen, J., and Hole, L.: Assessing the Impacts of Long-Range Sulfur and Nitrogen Deposition on Arctic and Sub-Arctic Ecosystems, *Ambio*, 39, 136–47, <https://doi.org/10.1007/s13280-010-0022-7>, 2010.
- Galmarini, S., Makar, P., Clifton, O. E., Hogrefe, C., Bash, J. O., Bellasio, R., Bianconi, R., Bieser, J., Butler, T., Ducker, J., Flemming, J., Hodzic, A., Holmes, C. D., Kioutsioukis, I., Kranenburg, R., Lupascu, A., Perez-Camanyo, J. L., Pleim, J., Ryu, Y.-H., San Jose, R., Schwede, D., Silva, S., and Wolke, R.: Technical note: AQMEII4 Activity 1: evaluation of wet and dry deposition schemes as an integral part of regional-scale air quality models, *Atmos. Chem. Phys.*, 21, 15663–15697, <https://doi.org/10.5194/acp-21-15663-2021>, 2021.
- Hazlett, P., Emilson, C., Lawrence, G., Fernandez, I., Ouimet, R., and Bailey, S.: Reversal of Forest Soil Acidification in the Northeastern United States and Eastern Canada: Site and Soil Factors Contributing to Recovery, *Soil Syst.*, 4, 3, <https://doi.org/10.3390/soilsystems4030054>, 2020.
- Hengl, T.: SoilGrids250m 2017-03 Absolute depth to bedrock (in cm), ISRIC – World Soil Inf., <https://data.isric.org/geonetwork/srv/api/records/f36117ea-9be5-4afd-bb7d-7a3e77bf392a> (last access: 3 June 2024), 2017.
- Hengl, T.: Clay content in % (kg/kg) at 6 standard depths (0, 10, 30, 60, 100 and 200 cm) at 250 m resolution (v0.2), Zenodo [data set], <https://doi.org/10.5281/zenodo.2525663>, 2018a.
- Hengl, T.: Coarse fragments % (volumetric) at 6 standard depths (0, 10, 30, 60, 100 and 200 cm) at 250 m resolution, Zenodo [data set], <https://doi.org/10.5281/zenodo.2525682>, 2018b.
- Hengl, T.: Sand content in % (kg / kg) at 6 standard depths (0, 10, 30, 60, 100 and 200 cm) at 250 m resolution (v0.2), Zenodo [data set], <https://doi.org/10.5281/zenodo.2525662>, 2018c.
- Hengl, T.: Soil bulk density (fine earth) 10 x kg/m-cubic at 6 standard depths (0, 10, 30, 60, 100 and 200 cm) at 250 m resolution (v0.2), Zenodo [data set], <https://doi.org/10.5281/zenodo.2525665>, 2018d.
- Hengl, T. and Wheeler, I.: Soil organic carbon content in x 5 g/kg at 6 standard depths (0, 10, 30, 60, 100 and 200 cm) at 250 m resolution (v0.2), Zenodo [data set], <https://doi.org/10.5281/zenodo.2525553>, 2018.
- Hijmans, R. J.: terra: Spatial Data Analysis. R package version 1.7-23, <https://CRAN.R-project.org/package=terra> (last access: 20 March 2023), 2023.
- Johnson, D. W. and Turner, J.: Nitrogen budgets of forest ecosystems: a review, *Forest Ecol. Manag.*, 318, 370–379, <https://doi.org/10.1016/j.foreco.2013.08.028>, 2014.
- Koseva, I. S., Watmough, S. A., and Aherne, J.: Estimating base cation weathering rates in Canadian forest soils using a simple texture-based model, *Biogeochemistry*, 101, 183–196, <https://doi.org/10.1007/s10533-010-9506-6>, 2010.
- Lawrence, G. B., David, M. B., Lovett, G. M., Murdoch, P. S., Burns, D. A., Stoddard, J. L., Baldigo, B. P., Porter, J. H., and Thompson, A. W.: Soil Calcium Status and the Response of Stream Chemistry to Changing Acidic Deposition Rates, *Ecol. Appl.*, 9, 1059–1072, [https://doi.org/10.1890/1051-0761\(1999\)009\[1059:SCSATR\]2.0.CO;2](https://doi.org/10.1890/1051-0761(1999)009[1059:SCSATR]2.0.CO;2), 1999.
- Lawrence, G. B., Hazlett, P. W., Fernandez, I. J., Ouimet, R., Bailey, S. W., Shortle, W. C., Smith, K. T., and Antidormi, M. R.: Declining Acidic Deposition Begins Reversal of Forest-Soil Acidification in the Northeastern U.S. and Eastern Canada, *Environ. Sci. Technol.*, 49, 13103–13111, <https://doi.org/10.1021/acs.est.5b02904>, 2015.
- Li, H. and McNulty, S. G.: Uncertainty analysis on simple mass balance model to calculate critical loads for soil acidity, *Environ. Pollut.*, 149, 315–26, <https://doi.org/10.1016/j.envpol.2007.05.014>, 2007.
- Liang, T. and Aherne, J.: Critical loads of acidity and exceedances for 1138 lakes and ponds in the Canadian Arctic, *Sci. Total Environ.*, 652, 1424–1434, <https://doi.org/10.1016/j.scitotenv.2018.10.330>, 2019.
- Likens, G. E., Driscoll, C. T., and Buso, D. C.: Long-term effects of acid rain: response and recovery of a forest ecosystem, *Science*, 272, 244–246, <https://doi.org/10.1126/science.272.5259.244>, 1996.
- Makar, P. A., Akingunola, A., Aherne, J., Cole, A. S., Aklilu, Y.-A., Zhang, J., Wong, I., Hayden, K., Li, S.-M., Kirk, J., Scott, K., Moran, M. D., Robichaud, A., Cathcart, H., Baratzedah, P., Pabla, B., Cheung, P., Zheng, Q., and Jeffries, D. S.: Estimates of exceedances of critical loads for acidifying deposition in Alberta and Saskatchewan, *Atmos. Chem. Phys.*, 18, 9897–9927, <https://doi.org/10.5194/acp-18-9897-2018>, 2018.
- Mandre, M., Kask, R., Pikk, J., and Ots, K.: Assessment of growth and stemwood quality of Scots pine on territory influenced by alkaline industrial dust, *Environ. Monit. Assess.*, 138, 51–63, <https://doi.org/10.1007/s10661-007-9790-3>, 2008.
- McDonnell, T. C., Phelan, J., Talhelm, A. F., Cosby, B. J., Driscoll, C. T., Sullivan, T. J., and Greaver, T.: Protection of forest ecosystems in the eastern United States from elevated atmospheric deposition of sulfur and nitrogen: A comparison of steady-state and dynamic model results, *Environ. Pollut.*, 318, 120887, <https://doi.org/10.1016/j.envpol.2022.120887>, 2023.
- McKenney, D., Papadopol, P., Campbell, K., Lawrence, K., Hutchinson, M., and others: Spatial models of Canada-and North America-wide 1971/2000 minimum and maximum temperature, total precipitation and derived bioclimatic variables, *Frontline Technical Note 106*, ISBN 0662404807, 2006.
- Mongeon, A., Aherne, J., and Watmough, S. A.: Steady-state critical loads of acidity for forest soils in the Geor-

- gia Basin, British Columbia, *J. Limnol.*, 69, 193–200, <https://doi.org/10.4081/jlimnol.2010.s1.193>, 2010.
- Moran, M. D., Savic-Jovcic, V., Makar, P. A., Gong, W., Stroud, C. A., Zhang, J., Zheng, Q., Chen, J., Akingunola, A., Lupu, A., Ménard, S., Menelaou, K., and Munoz-Alpizar, R.: Operational chemical weather forecasting with the ECCO online Regional Air Quality Deterministic Prediction System version 023 (RAQDPS023) – Part 1: System description, *Geosci. Model. Dev.*, in preparation, 2025a.
- Moran, M. D., Lupu, A., Savic-Jovcic, V., Zhang, J., Zheng, Q., Boutzis, E., Mashayekhi, R., Stroud, C. A., Ménard, S., Chen, J., Menelaou, K., Munoz-Alpizar, R., Kornic, D., and Manseau, P.: Operational chemical weather forecasting with the ECCO online Regional Air Quality Deterministic Prediction System version 023 (RAQDPS023) – Part 2: Prospective and retrospective performance evaluations, *Geosci. Model. Dev.*, in preparation, 2025b.
- Murray, C. A., Whitfield, C. J., and Watmough, S. A.: Uncertainty-based terrestrial critical loads of nutrient nitrogen in northern Saskatchewan, Canada, *Boreal Environ. Res.*, 22, 231–244, 2017.
- Myers-Smith, I. H., Kerby, J. T., Phoenix, G. K., Bjerke, J. W., Epstein, H. E., Assmann, J. J., John, C., Andreu-Hayles, L., Angers-Blondin, S., Beck, P. S., and Berner, L. T.: Complexity revealed in the greening of the Arctic, *Nat. Clim. Change*, 10, 106–117, <https://doi.org/10.1038/s41558-019-0688-1>, 2020.
- NADP: National Trends Network, National Atmospheric Deposition Program (NRSP-3), NADP Program Office, Wisconsin State Laboratory of Hygiene, 465 Henry Mall, Madison, WI 53706, <https://nadp.slh.wisc.edu/networks/national-trends-network> (last access: 3 June 2024), 2023.
- National Wetlands Working Group: The Canadian Wetland Classification System, 2nd ed, edited by: Warner, B. G. and Rubec, C. D. A., National Wetlands Working Group, Wetlands Research Branch, University of Waterloo, Waterloo, ON, Canada, ISBN 0-662-25857-6, 1997.
- NEG-ECP: Critical Load of Sulphur and Nitrogen Assessment and Mapping Protocol for Upland Forests, N. Engl. Gov. East. Can. Prem. Environ. Task Group Acid Rain Action Plan Halifax N. S., 2001.
- Nilsson, J. and Grenfelt, P.: Critical loads for sulphur and nitrogen, Nordic Council of Ministers, Copenhagen, Denmark, ISBN 87-7303-249-2, 1988.
- Ouimet, R., Duchesne, L., Houle, D., and Arp, P.: Critical Loads and Exceedances of Acid Deposition and Associated Forest Growth in the Northern Hardwood and Boreal Coniferous Forests in Québec, Canada, *Water Air Soil Pollut. Focus*, 1, 119–134, <https://doi.org/10.1023/A:1011544325004>, 2001.
- Ouimet, R., Arp, P. A., Watmough, S. A., Aherne, J., and DeMerchant, I.: Determination and Mapping Critical Loads of Acidity and Exceedances for Upland Forest Soils in Eastern Canada, *Water Air Soil Pollut.*, 172, 57–66, <https://doi.org/10.1007/s11270-005-9050-5>, 2006.
- Paal, J., Degtjarenko, P., Suija, A., and Liira, J.: Vegetation responses to long-term alkaline cement dust pollution in inus sylvestris-dominated boreal forests – niche breadth along the soil pH gradient, *Appl. Veg. Sci.*, 16, 248–259, <https://doi.org/10.1111/j.1654-109X.2012.01224.x>, 2013.
- Pardo, L. H., Duarte, N., Miller, E. K., and Robin-Abbott, M.: Tree chemistry database (version 1.0), USDA For. Serv. Northeast. Res. Stn., 324, <https://doi.org/10.2737/NE-GTR-324>, 2005.
- Pardo, L. H., Coombs, J. A., Robin-Abbott, M. J., Pontius, J. H., and D'Amato, A. W.: Tree species at risk from nitrogen deposition in the northeastern United States: A geospatial analysis of effects of multiple stressors using exceedance of critical loads, *Forest Ecol. Manag.*, 454, 117528, <https://doi.org/10.1016/j.foreco.2019.117528>, 2019.
- Paré, D., Bernier, P., Lafleur, B., Titus, B. D., Thiffault, E., Maynard, D. G., and Guo, X.: Estimating stand-scale biomass, nutrient contents, and associated uncertainties for tree species of Canadian forests, *Can. J. Forest Res.*, 43, 599–608, <https://doi.org/10.1139/cjfr-2012-0454>, 2013.
- Park, S. H., Gong, S. L., Gong, W., Makar, P. A., Moran, M. D., Zhang, J., and Stroud, C. A.: Relative impact of windblown dust versus anthropogenic fugitive dust in PM_{2.5} on air quality in North America, *J. Geophys. Res.-Atmos.*, 115, D16210, <https://doi.org/10.1029/2009JD013144>, 2010.
- Posch, M., de Smet, P. A. M., Hettelingh, J.-P., and Downing, R. J.: Calculation and Mapping of Critical Thresholds in Europe: Status Report 1999, Coordination Center for Effects, National Institute of Public Health and the Environment, Bilthoven, Netherlands, ISBN 90-6960-083-8, 1999.
- Posch, M., de Vries, W., and Sverdrup, H. U.: Mass Balance Models to Derive Critical Loads of Nitrogen and Acidity for Terrestrial and Aquatic Ecosystems, in: Critical Loads and Dynamic Risk Assessments: Nitrogen, Acidity and Metals in Terrestrial and Aquatic Ecosystems, edited by: de Vries, W., Hettelingh, J.-P., and Posch, M., Springer Netherlands, Dordrecht, 171–205, https://doi.org/10.1007/978-94-017-9508-1_6, 2015.
- Pribyl, D. W.: A critical review of the conventional SOC to SOM conversion factor, *Geoderma*, 156, 75–83, <https://doi.org/10.1016/j.geoderma.2010.02.003>, 2010.
- QGIS Development Team: QGIS Geographic Information System, Open Source Geospatial Foundation Project, <http://qgis.osgeo.org> (last access: 22 January 2023), 2023.
- R Core Team: R: A Language and Environment for Statistical Computing, Vienna, Austria, <https://www.R-project.org/> (last access: 20 March 2023), 2021.
- Radke, L., Hegg, D., Lyons, J., Brock, C., Hobbs, P., Weiss, R., and Rasmussen, R.: Airborne measurements on smokes from biomass burning, in: Aerosols and Climate, edited by: Hobbs, P. V. and McCormick, M. P., A. Deepak Publishing Co., Hampton, VA, 411–422, 1988.
- Radke, L. F., Lyons, J. H., Hobbs, P. V., Hegg, D. A., Sandberg, D. V., and Ward, D. E.: Airborne monitoring and smoke characterization of prescribed fires on forest lands in western Washington and Oregon, US Department of Agriculture, Forest Service, Pacific Northwest Research Station, <https://doi.org/10.2737/PNW-GTR-251>, 1990.
- Reinds, G. J., Posch, M., Aherne, J., and Forsius, M.: Assessment of Critical Loads of Sulphur and Nitrogen and Their Exceedances for Terrestrial Ecosystems in the Northern Hemisphere, in: Critical loads and dynamic risk assessments: Nitrogen, acidity and metals in terrestrial and aquatic ecosystems, edited by: De Vries, W., Hettelingh, J.-P., and Posch, M., Springer, 403–418, https://doi.org/10.1007/978-94-017-9508-1_15, 2015.

- Reinds, G. J., Thomas, D., Posch, M., and Slootweg, J.: Critical loads for eutrophication and acidification for European terrestrial ecosystems, Umweltbundesamt, Wörlitzer Platz 1, 06844 Dessau-Roßlau, Germany, ISSN 1862-4804, 2021.
- Rosen, K., Gundersen, P., Tegnhammar, L., Johansson, M., and Frogner, T.: Nitrogen enrichment of Nordic forest ecosystems: the concept of critical loads, *Ambio*, 21, 364–368, 1992.
- Shangguan, W., Hengl, T., Mendes de Jesus, J., Yuan, H., and Dai, Y.: Mapping the global depth to bedrock for land surface modeling, *J. Adv. Model. Earth Sy.*, 9, 65–88, <https://doi.org/10.1002/2016MS000686>, 2017.
- Simkin, S. M., Allen, E. B., Bowman, W. D., Clark, C. M., Belnap, J., Brooks, M. L., Cade, B. S., Collins, S. L., Geiser, L. H., Gilliam, F. S., Jovan, S. E., Pardo, L. H., Schulz, B. K., Stevens, C. J., Suding, K. N., Throop, H. L., and Waller, D. M.: Conditional vulnerability of plant diversity to atmospheric nitrogen deposition across the United States, *P. Natl. Acad. Sci. USA*, 113, 4086–4091, <https://doi.org/10.1073/pnas.1515241113>, 2016.
- Skeffington, R., Whitehead, P., and Abbott, J.: Quantifying uncertainty in critical loads: (B) Acidity mass balance critical loads on a sensitive site, *Water Air. Soil Pollut.*, 169, 25–46, <https://doi.org/10.1007/s11270-006-2218-9>, 2006.
- SLCWG: Soil landscapes of Canada version 3.2, Soil Landscapes of Canada Working Group. Agriculture and Agri-Food Canada, <https://sis.agr.gc.ca/cansis/nsdb/slc/v3.2/index.html> (last access: 3 June 2024), 2010.
- Statistics Canada: Agricultural ecumene boundary file, 2016 Census of Agriculture, Statistics Canada, Cat. No 92-639-X, <https://www150.statcan.gc.ca/> (last access: 20 March 2023), 2017.
- Sverdrup, H. and De Vries, W.: Calculating critical loads for acidity with the simple mass balance method, *Water. Air. Soil Pollut.*, 72, 143–162, <https://doi.org/10.1007/BF01257121>, 1994.
- Sverdrup, H. and Warfvinge, P.: The effect of soil acidification effect on the growth of trees, grass and herbs, as expressed by the $(Ca + Mg + K)/Al$ ratio, Reports in ecology and environmental engineering, Lund University Department of Chemical Engineering II, ISSN 1104-2877, 1993.
- Tegen, I. and Fung, I.: Contribution to the atmospheric mineral aerosol load from land surface modification, *J. Geophys. Res.-Atmos.*, 100, 18707–18726, <https://doi.org/10.1029/95JD02051>, 1995.
- Tol, P.: Colour schemes, SRON Technical Note, Doc. no. SRON/EPS/TN/09-002, <https://personal.sron.nl/~pault/> (last access: 10 January 2025), 2012.
- Vandinther, N. and Aherne, J.: Biodiversity-Based Empirical Critical Loads of Nitrogen Deposition in the Athabasca Oil Sands Region, *Nitrogen*, 4, 169–193, <https://doi.org/10.3390/nitrogen4020012>, 2023a.
- Vandinther, N. and Aherne, J.: Ecological Risks from Atmospheric Deposition of Nitrogen and Sulphur in Jack Pine forests of Northwestern Canada, *Nitrogen*, 4, 102–124, <https://doi.org/10.3390/nitrogen4010008>, 2023b.
- Whitfield, C. J., Aherne, J., Watmough, S. A., and McDonald, M.: Estimating the sensitivity of forest soils to acid deposition in the Athabasca Oil Sands Region, Alberta, *J. Limnol.*, 69, 201–208, <https://doi.org/10.4081/jlimnol.2010.s1.201>, 2010.
- Wilkins, K., Cathcart, H., Hickey, P., Hanley, O., Vintró, L. L., and Aherne, J.: Influence of Precipitation on the Spatial Distribution of ^{210}Pb , ^{7}Be , ^{40}K and ^{137}Cs in Moss, *Pollutants*, 3, 102–113, <https://doi.org/10.3390/pollutants3010009>, 2023.
- Williston, P., Aherne, J., Watmough, S., Marmorek, D., Hall, A., de la Cueva Bueno, P., Murray, C., Henolson, A., and Laurence, J. A.: Critical levels and loads and the regulation of industrial emissions in northwest British Columbia, Canada, *Atmos. Environ.*, 146, 311–323, <https://doi.org/10.1016/j.atmosenv.2016.08.058>, 2016.
- Wu, W. and Driscoll, C. T.: Impact of Climate Change on Three-Dimensional Dynamic Critical Load Functions, *Environ. Sci. Technol.*, 44, 720–726, <https://doi.org/10.1021/es900890t>, 2010.
- Zhao, W., Zhao, Y., Ma, M., Chang, M., and Duan, L.: Long-term variability in base cation, sulfur and nitrogen deposition and critical load exceedance of terrestrial ecosystems in China, *Environ. Pollut.*, 289, 117974, <https://doi.org/10.1016/j.envpol.2021.117974>, 2021.